SAPIENZA
UNIVERSITÀ DI ROMA

Yeast decapping mutants as model systems for ageing and autophagy

Faculty of Mathematical, Physical and Natural Science
Department of Biology and Biotechnology "Charles Darwin"
PhD course in Cell and Developmental Biology
XXXVI Cycle

2022/2023

PhD student
Benedetta Caraba

Supervisor
Prof. Cristina Mazzoni

Internal reviewer
Prof. Rodolfo Negri

Coordinator
Prof. Simone Ferrari

Index

1. Summary

The *S. cerevisiae* yeast has been successfully established over time as a useful eukaryotic model for the study of various physiological and pathological cellular processes. Among these, cellular ageing plays a role of great interest, as it is the result of the occurrence of different pathways and molecular changes which can be challenging to study in a more complex model system. In previous studies it has been shown that the mutant strain for the essential gene *LSM4*, whose protein product is involved in the degradation of messenger RNAs, shows premature markers of aged cells and shorter life span due to the uncontrolled accumulation of RNA in the cytoplasm. In this context, generally the survival mechanism of choice of the cell population turns out to be autophagy and, if this is not sufficient, the consequent triggered process is the regulated cell death. It has been demonstrated the involvement of LSM complex in autophagy regulation and in the case of the *LSM4* mutant, a gene involved in the biosynthesis of phospholipids and membranes necessary for the autophagic process, *NEM1*, has a positive effect on the life span of the strain. Starting from this, in the present work we demonstrate that in the mutant strain the activation of autophagy due to restriction of nutrients or during chronological ageing is compromised, with an accumulation of cytoplasmic autophagosomal structures, and that the increase in viability under calorie restriction is probably dependent on a change in RNAs metabolism or in the activation of an alternative autophagic pathway. Furthermore, we created a reporter system comprising the truncated form of *LSM4* and the GFP protein at genome level using the CRISPR/Cas9 system, which shows the phenotypic markers of premature aged cells as well.

2. Synopsis of the work

The multifactorial process of ageing, of great interest for the human health, can be challenging to study due to the intricate pathways and networks involved that include both genetic and environmental factors. In this regard, the use of a simple unicellular model system like *Saccharomyces cerevisiae* can give us a great number of informations that can be easily transposed in higher eukaryotes. In fact, it is now well established that yeast cells can undergo a physiological ageing characterized by the onset of specific regulated cell death markers (Madeo, Fröhlich and Fröhlich, 1997), and other processes that mediate the survival and the cellular homeostasis are conserved from yeast to human. Among these, the autophagy process plays an essential role in the degradation and recycle of damaged parts of the cell (proteins, nucleic acid, entire organelles and more) in order to restore the cellular homeostasis and promote the elongation of the life span (Klionsky and Emr, 2000; Ryter, Cloonan and Choi, 2013), and misregulations of this process are associated with various human diseases, such as neurodegenerative diseases and cancer (Daniel J Klionsky *et al.*, 2021).

In yeast, the regulation of the autophagy triggered by nutrient stress occurs post-transcriptionally: the autophagy related genes (*ATG*) mRNAs are rapidly degraded through decapping and 5'-3' degradation during nutrient rich conditions, while they are stabilized and translated under nutrient restriction, mediating the induction of the autophagic pathway. The stabilization of *ATG* mRNAs is due to the inactivation of the decapping process through the inhibition of the Tor Complex 1, one of the main regulators of nutrient sensing stress (Hu *et al.*, 2015). Interestingly, recent studies revealed that positive regulators of the decapping process like Dhh1 and the Pat1/Lsm complex are important for the expression and 3' protection of a subset of *ATG* genes, revealing a dual role for this machinery in regulating the autophagic process (Tharun *et al.*, 2005; Gatica *et al.*, 2019; Liu *et al.*, 2019). Therefore, we focused our work on the relation between the autophagy and the decapping processes.

The yeast model system of our choice is a strain expressing a truncated form of the Lsm4 protein, a component of the heptameric ring LSM. The strain ages prematurely, as the decapping process is impaired and mRNAs accumulate in the cytoplasm, favouring a strong accumulation of reactive species of oxygen that concurs to its short life span. Another interesting phenotype is the high sensitivity to autophagy-inducing compounds like caffeine and rapamycin, suggesting a defect in this process. The hypothesis was confirmed by Western Blot analysis where the fusion protein GFP-Atg8 was used to track the autophagic flux: despite the high production of the chimerical protein in nitrogen starvation condition, the degradation of the Atg8 part was not efficient. Examining the cells at the fluorescent microscope, we noticed a great accumulation of GFP dots in the cytoplasm, representing the autophagosomal structures, during ageing and under nitrogen starvation, suggesting a problem in a later stage of autophagosomes internalization. This was also true for another mutant in a component the cytoplasmic LSM complex, *lsm1Δ*, reinforcing the

hypothesis that mutations in the decapping regulation could lead to problems in the autophagic pathway.

Interestingly, when we tested the viability of the strain in different types of nutrient restrictions, we found out that nitrogen starvation was detrimental as expected, while glucose restriction led to an incredible elongation of the life span, in both mutant and wild type strains. As it is now well established that a dietary restriction can extend the life expectancy both in yeast and human (Fontana, Partridge and Longo, 2010), this result obtained in a mutant defective in the autophagic process could be of great interest. In fact, the resulted elongation of life span could be due to the activation of other stress-responsive pathways, such as the activation of the NAD-dependent deacetylase Sir2, of which has been demonstrated the involvement in the regulation of mitophagy (Okamoto, Kondo-Okamoto and Ohsumi, 2009; Sampaio-Marques *et al.*, 2012) together with its well characterized action in the repression of rDNA recombination that is able to increase the fitness and life span of yeast cells (Kaeberlein, McVey and Guarente, 1999). Moreover, when cultured in water we saw an increase of extracellular RNA compared to the SD medium and the wild type, without any cellular mass decrease, suggesting that in extreme calorie restriction the secretion of RNAs in the extracellular environment could represent an additional survival mechanism. Future perspectives would therefore analyse the hypothesis that the regulation of the energy-stress mediated autophagy could differ from the one promoted by nitrogen and aminoacids deprivation, and the possible involvement of a regulated secretion in the elongation of the life span.

In addition, we constructed the *lsm4Δ1* mutant at genome level with the CRISPR/Cas9 technique and the spot test assays revealed the same high sensitivity to caffeine and rapamycin previously described for the MCY4 strain, confirming the possibility to use the engineered strain as model system for future studies.

3. Introduction

The yeast *Saccharomyces cerevisiae* has been chosen from decades as a model system thanks to its simple maintenance and manipulation together with its incredibly high level of conservation of higher eukaryotic processes and features, and its use has improved and simplified the study of physiological and pathological conditions. The complex and dynamic process of ageing, that can be challenging to investigate due to the intricate pathways and networks involved that include both genetic and environmental factors, can be easily studied in this unicellular organism. In fact, it is now well established that yeast cells can undergo a physiological ageing characterized by the onset of specific regulated cell death markers found also in higher eukaryotes, such as phosphatidylserine externalization and chromatin condensation and fragmentation (Madeo, Fröhlich and Fröhlich, 1997). During ageing the cellular homeostasis and viability are maintained and restored from stressful conditions thanks to the activation of different pro-survival processes, and central among these is the autophagic process. Autophagy, more precisely macroautophagy, is a highly conserved process that mediates the remodelling of intracellular membranes in order to sequester portion of cytoplasm to be delivered and degraded inside specific compartments, such as lysosomes in mammals and vacuole in plants and yeast (Klionsky and Emr, 2000), promoting in this way the clearance of damaged organelles, proteins and macromolecules through specific degradation and recycle of the components (Ryter, Cloonan and Choi, 2013). Autophagy plays an essential role also in starvation adaptation of the cells, as it is stimulated by the inactivation of the kinase Tor, a conserved signal of nutrient deprivation (Noda and Ohsumi, 1998). In yeast, the link between starvation and the extension of lifespan is well known (Fabrizio and Longo, 2003; Goldberg *et al.*, 2009), and in the last years it became clear that the autophagic process is connected to mRNAs degradation (Delorme-Axford and Klionsky, 2019). Therefore, in this work we explored the role of a mutant in the decapping process during the starvation stimulated autophagy.

The LSM (like-Sm) protein family is a group of evolutionarily conserved proteins from bacteria to yeast and humans (Wilusz and Wilusz, 2013) involved in the regulation of mRNA splicing, stability and translation (He and Parker, 2000) (Figure 1). *LSM4* is an essential gene and the protein product Lsm4 is a component of both nuclear and cytoplasmic LSM complexes, and we previously reported that is involved in ageing and apoptosis in the yeast *Saccharomyces cerevisiae*. In fact, the expression of a truncated protein of the KlLsm4 from the related yeast *Kluyveromyces lactis* (*Kllsm4Δ1*), lacking the C-terminal Q/N-rich domain, leads to premature ageing of the cells and they undergo regulated cell death (Mazzoni, Mancini, Madeo, *et al.*, 2003; Mazzoni, Mancini, Verdone, *et al.*, 2003) due to the accumulation of mRNAs in the cytoplasm which in turn increases the cell sensitivity to stress stimuli, such as oxidative stress, while the splicing process is unaffected. Therefore it demonstrated that the C-terminal Q/N-rich domain of *KlLSM4* is needed for efficient RNA degradation (Mazzoni, Mancini, Verdone, *et al.*, 2003; Mazzoni *et al.*, 2005) and for Processing-bodies (P-bodies) localization (Mazzoni, D'Addario and Falcone, 2007; Reijns *et al.*,

2008), while others reported that this region of *ScLSM4* is important only together with the Edc3 protein (Decker, Teixeira and Parker, 2007). On the other hand, the C-terminal domain of the human Lsm4 consists of an arginine-glycine-glycine repeat (RGG) and similarly to the yeast counterpart it plays and important role in P-bodies accumulation, while it is not required for the association to the Lsm1-7 complex, as observed in yeast instead (Kato *et al.*, 2012; Arribas-Layton *et al.*, 2016). In addition, of great interest for the medical field, the human *LSM4* gene has also been found to be misregulated in different types of cancer where its over-expression is associated with poor prognosis (Chen *et al.*, 2021; Ta *et al.*, 2021; Sun, Tan and Peng, 2022).

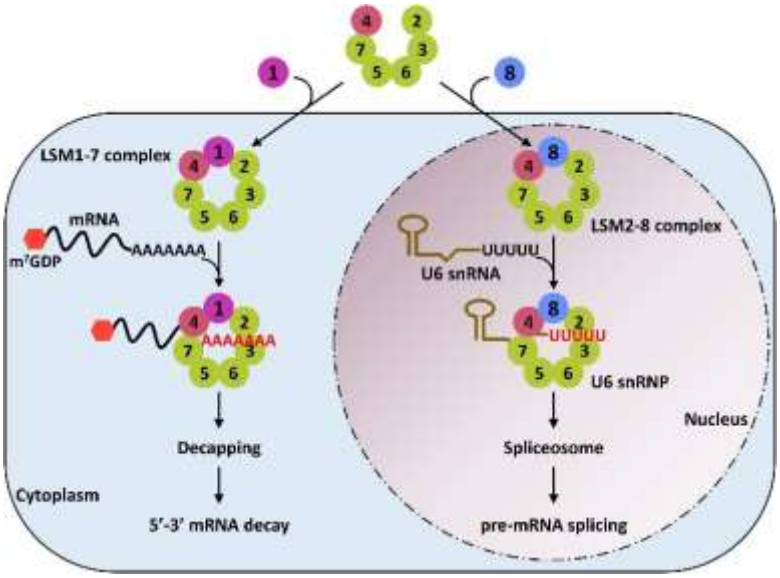

Figure 1. The LSM complexes are involved in the decapping process and mRNAs degradation that occurs in the cytoplasm (LSM1-7) and in the splicing process (LSM2-8) in the nucleus. The LSM4 protein (in red) takes part of both complexes. Adapted from (Catalá *et al.*, 2019).

Recent studies revealed the involvement of Lsm proteins in the autophagic process (Costanzo *et al.*, 2010; Mazzoni and Falcone, 2011; Mitchell *et al.*, 2013), and in a previous work we found that one of the multicopy extragenic suppressor of the premature ageing phenotype of the *Kllsm4Δ1* expressing strain is the Nuclear Envelope Morphology protein 1 (*NEM1*), which is involved in the biosynthesis of phospholipids and in nuclear and ER morphology. The overexpression of this protein suppresses most of the apoptotic phenotypes of the mutant, such as the nuclear and ER aberrant morphology, and reduces the oxidative stress sensitivity (Palermo *et al.*, 2015). The Nem1 protein, together with its regulatory subunit Spo7 and their target Pah1/lipin, is important for the autophagic process triggered by nutrient starvation and TORC1 inactivation (Rahman, Mostofa and Ushimaru, 2018). In addition, other studies demonstrated that in cells lacking the RNA helicase Dhh1 or the decapping protein Dcp2, the autophagy was increased despite the high levels

of nutrients in the medium (Hu *et al.*, 2015). This is due to the impairment in the regulation of the *ATG* genes (autophagy-related genes) at post-transcriptional level: in nutrient rich conditions, TORC1 is able to phosphorylate a serine residue on the Dcp2 protein, which in turn promotes the association of the RCK-Dhh1 complex to *ATG* mRNAs and their subsequent decapping and degradation by the exoribonuclease Xrn1 (Hu *et al.*, 2015); on the other hand, when nutrients are scarce and in starvation conditions, the activity of TORC1 is reduced, leading to a lower level of Dcp2 phosphorylation and decapping activity that promotes the stabilization of *ATG* mRNAs (Figure 2).

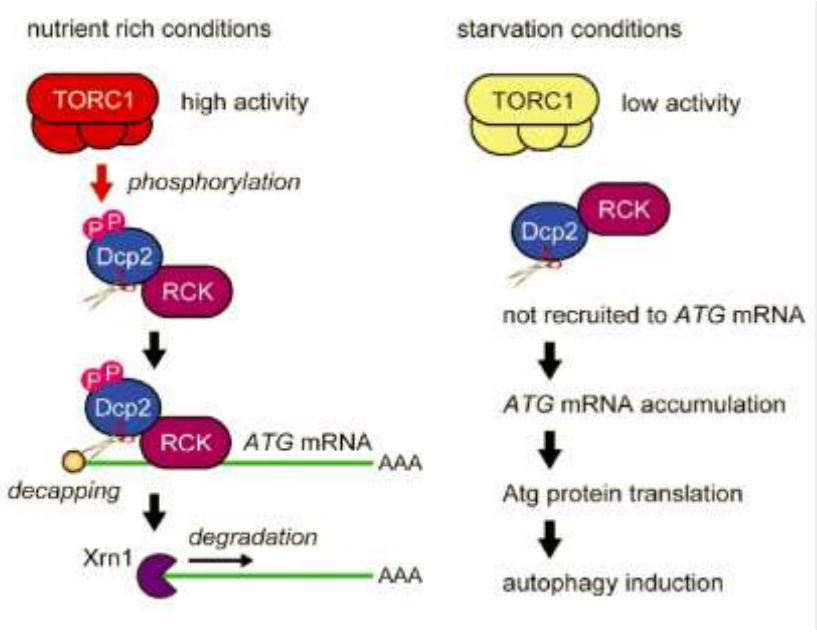

Figure 2. The regulation of the *ATG* genes occurs at post-transcriptional level. The nutrient conditions regulate the activity of TORC1 which in turn controls the activity of the decapping machinery (Dcp2/RCK), resulting in the degradation or stabilization of *ATG* transcripts (Nakatogawa, 2015).

Interestingly, recent studies demonstrated the dual role of Dhh1 in the autophagy process, as its deletion leads to lower survival of the cells during prolonged nitrogen starvation (Liu *et al.*, 2019). The mentioned research proposes a model where Dhh1 would coordinate the degradation of *ATG* mRNAs under nutrient-rich conditions, while upon nitrogen starvation it would facilitate the autophagic process by promoting the translation of *ATG1* and *ATG13* mRNAs (Liu *et al.*, 2019). Similarly, the deadenylation complex CCR4/NOT has been found to promote the degradation of a subset of *ATG* mRNAs when the cells have access to an abundance of nutrients, while it can promote the expression of a different subset of *ATG* genes involved in the autophagy induction under starvation conditions (Yin *et al.*, 2023). Regarding the role of the LSM complex in this

context, it is known that its interaction with the RNA-binding protein Pat1 is needed for the binding to the 3′ untranslated region (UTR) of oligoadenylated mRNAs (Chowdhury, Mukhopadhyay and Tharun, 2007; Chowdhury, Kalurupalle and Tharun, 2014) and for their subsequent decapping and degradation. Interestingly, the Pat1/Lsm complex is also important for the protection of the 3′ end of mRNAs from the exosome-dependent 3′-5′ degradation (He and Parker, 2001; Tharun *et al.*, 2005), and this feature is critical for the stabilization of a subset of *ATG* mRNAs that promotes the activation of the autophagic process (Gatica *et al.*, 2019) (Figure 3).

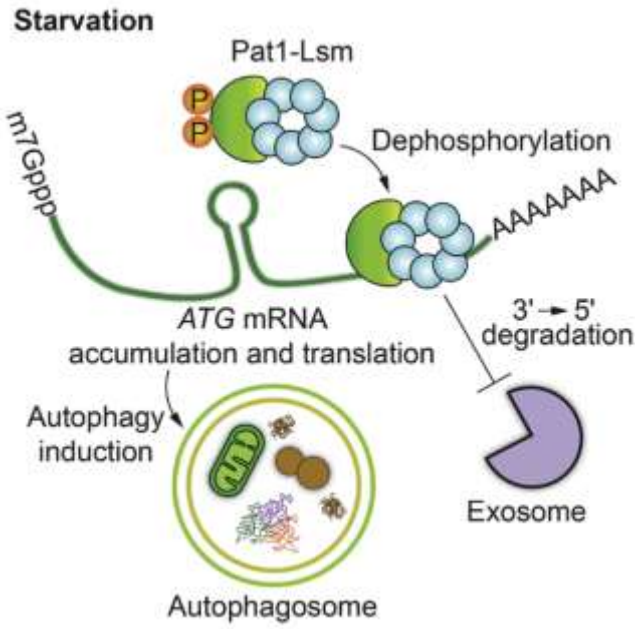

Figure 3. During starvation, the Pat1/Lsm complex is important for the 3′ protection of *ATG* transcripts from the exosome degradation, which ensures the Atg translation and autophagy induction (Gatica *et al.*, 2019).

The autophagy activation is also important for the elongation of eukaryotic life span during calorie restriction (Fontana, Partridge and Longo, 2010), via TOR inhibition by the AMPK/SNF1 kinases cascade (Gwinn *et al.*, 2008) and activation of sirtuins, such as Sir2. In yeast, the Silent Information Regulator 2 (*SIR2*) is a histone deacetylase involved in cellular homeostasis through rDNA recombination inhibition, telomere, HML and HMR silencing and its functionality is strictly dependent on the oxidative state of the cell. In calorie restriction, the concentration of its cofactor NAD+ is sufficient to enhance its deacetylation activity and the toxic accumulation of extrachromosomal rDNA circles (ERCs) is repressed, promoting the wellness of the cell with a final outcome of increased life span (Kaeberlein, McVey and Guarente, 1999). Moreover, several studies demonstrated its involvement in the activation of autophagy in such condition, which again has a

positive action on the life span of the organism (Medvedik *et al.*, 2007; Morselli *et al.*, 2010; Sampaio-Marques *et al.*, 2012).

This doctoral research project starts from the acquired knowledge about the connection between the autophagy and the decapping processes and aims to investigate the role of the *LSM4* gene in this complex network, and to further expand the research to other Lsm protein.

4. Aims of the work

The use of the *Saccharomyces cerevisiae* yeast has simplified the study of a large variety of complex eukaryotic mechanisms, and it is now established as a model system for cellular ageing and related diseases important for human health. One of the main pathways involved in cellular survival during later stages of growth is autophagy, and recent studies demonstrated the dual role of the decapping machinery in its regulation (Gatica *et al.*, 2019; Liu *et al.*, 2019). Therefore, the use of mutant yeast strain in a component of the LSM complex, *lsm4Δ1,* could be relevant for the investigation of the relation between these two essential processes.

Firstly, we decided to express in the MCY4 strain the *S. cerevisiae* homologous gene *Sclsm4Δ1,* as the previous works of our research group were made using the *Kluyveromyces lactis* form. In order to ensure the viability of the strain while compromising the decapping process as desired, the *Sclsm4Δ1* protein is truncated at the 82 aspartic acid, while the full-length protein is 188 aminoacid long. In this way, we excluded the C-terminal Q/N-rich domain essential for the association with the decapping machinery, while the two N-terminal Sm-like domains were maintained and the association with the U6 snRNA and the splicing complex remained possible. After the validation of our new yeast model system for ageing, we focused our work on the study of the autophagy induction predominantly under nitrogen starvation, as it is a well-known strong inducer of this pathway (Takeshige *et al.*, 1992; Cebollero and Reggiori, 2009), and during calorie restriction. The autophagic flux and autophagosome localization were mainly assessed by Western Blot analysis and fluorescent microscopy using the fusion protein GFP-Atg8 as described in (Daniel J. Klionsky *et al.*, 2021), where the scientific community provides an exhaustive guide on the methods used in the autophagy evaluation in eukaryotic systems. The consequences of nitrogen and glucose starvation on the life span of cells were assessed by viability assays, while the sensitivity to autophagy-inducing molecules was performed by spot test analysis. Moreover, supernatants RNA content was evaluated during extreme calorie restriction, to evaluate a new possible survival process for the RNA-accumulating strain MCY4/*Sclsm4Δ1.*

Working with plasmid transformed yeasts could be misleading, as the trans-gene expression could not represent the physiological scenario, and the dependence on auxotrophic or antibiotic selection is a known limit of the technique. To overcome these issues, and create a reporter system for the truncated *lsm4Δ1* protein of which antibodies are not available, we created the *lsm4Δ1*-GFP mutant at genomic level using the genome editing system CRISPR/Cas9 optimised by (Stovicek, Borodina and Forster, 2015). The conserved phenotypes from the plasmid-expressing and the genome mutant strains would give us the opportunity to transpose the acquired knowledge on the behaviour in autophagy inducing conditions to this new promising model system, which could act as a platform of great interest for the discovery of new potential therapeutic targets for ageing and autophagy-related diseases.

5. Results

5.1 The *Sclsm4Δ1* mutant shows premature ageing and regulated cell death similar to *Kllsm4Δ1*

The yeast strain model of ageing of choice in our laboratory has been for many years the *S. cerevisiae* strain MCY4, which carries the *LSM4* essential gene under *Gal1-10* promoter control, transformed with a *K. lactis* truncated form of the protein (*Kllsm4Δ1*) on the centromeric pRS313 plasmid to allow the growth on glucose as a carbon source. The truncated protein comprises the first 72 aminoacids out of the 183 aa of the full-length protein, therefore it lacks the C-terminal Q/N-rich sequence needed for the regulation of the decapping machinery, resulting in premature loss of viability and early onset of regulated cell death markers, such as nuclei fragmentation and high sensitivity to reactive species of oxygen (ROS) (Mazzoni, Mancini, Madeo, *et al.*, 2003; Mazzoni, Mancini, Verdone, *et al.*, 2003). To mimic a more physiological scenario, we cloned the N-terminal domain of the *S. cerevisiae LSM4* gene, encoding the first 82 aminoacids out of the 188 aminoacids of the full-length protein, into the plasmid pRS313 and create the *Sclsm4Δ1* strain, which is now the main object of our experiments. As reported in Figure 4, panels A and B, although the viability on glucose is restored, the growth of the *Sclsm4Δ1* strain is slightly slower than the isogenic wild type strain CML39-11A and the MCY4 strain expressing on the same plasmid the full-length Lsm4 protein. This growth slowdown is not due to a lower expression of *Sclsm4Δ1* gene that, on the contrary, is highly expressed (Figure 4, panel C).

A

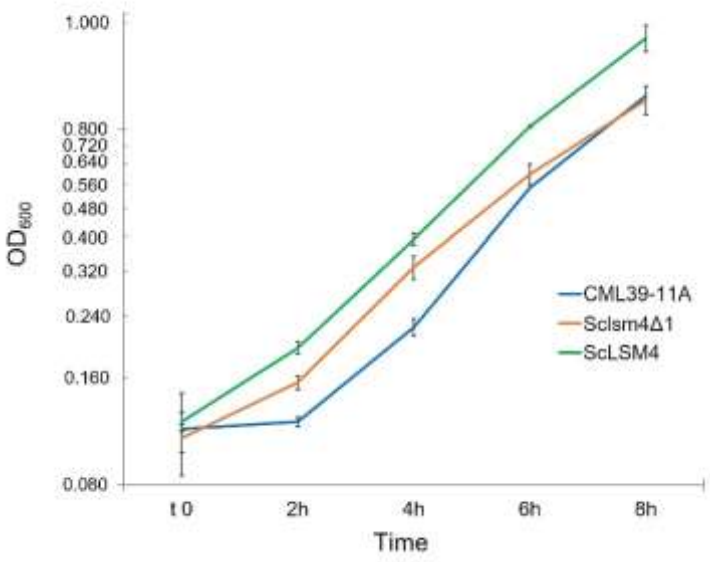

B

Strain	Growth rate (μ)
CML39-11A	0,375519 ± 0.105
MCY4/*Sclsm4Δ1*	0,270481 ± 0.042
MCY4/*ScLSM4*	0,326280 ± 0.056

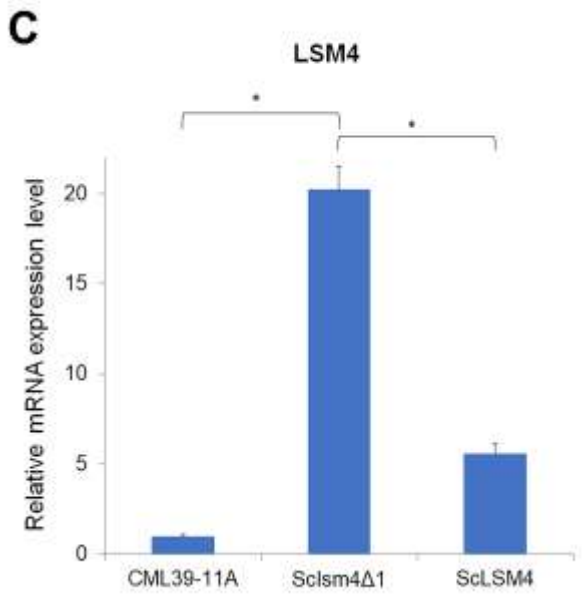

Figure 4. Growth curves relative to MCY4/*Sclsm4Δ1,* MCY4/*ScLSM4* and the wild type strain CML39-11A. **(A)** Strains were exponentially growing in YPD medium and OD_{600} values were taken every two hour. Error bars represent standard deviation of three independent biological replicates. **(B)** Growth rates (μ) of the strains of interest was calculated as $(\ln N_t - \ln N_0)/(t - t_0)$ in the intervals 4h-6h and 6h-8h. The mean and standard deviation of three independent replicates is reported. **(C)** Relative mRNA expression of *LSM4* in the strain of interest. The housekeeping gene TDH3 was used as the calibrator. The mean of the fold change (expressed as $2^{-\Delta\Delta Ct}$) of two biological replicate was plotted. Error bars represent standard deviation. *p-value<0.05.

Regarding the long-term viability during the stationary phase, known as Chronological Life Span (CLS), the *Sclsm4Δ1* strain shows a very short lifespan, with a total loss of viability on day 7, similar to that described for the *Kllsm4Δ1* strain, while the expression of the full-length Lsm4 protein restores the viability at wild type level, as both loss viability on day 14 (Figure 5). This result confirms that the short lifespan of the mutant is due to the truncation of the *Saccharomyces cerevisiae* Lsm4 protein.

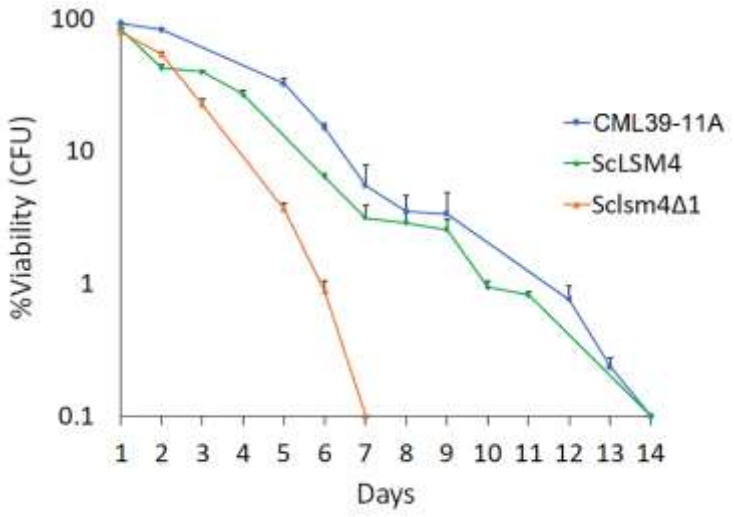

Figure 5. Chronological Life Span (CLS) of the wild type strain (CML39-11A) and MCY4 expressing *Sclsm4Δ1* mutant or the full length LSM4 protein (*ScLSM4*) cells cultured in Synthetic-defined medium (SD). Data are represented as the mean of three independent experiments ± standard deviation.

We then analysed the nuclei morphology and intracellular ROS production and accumulation by fluorescent microscopy to evaluate the similarity in phenotypes with the *Kllsm4Δ1* strain. As shown in Figure 6, panel A and B, the 4,6-diamidino-2-phenylindole (DAPI) stained nuclei are highly fragmented, enlarged and diffused in more than 15% of exponentially growing cells and in almost 40% of cells during stationary phase, representing a notable marker of regulated cell death. These percentages are much higher compared to the wild type, in which the percentage of cells with fragmented nuclei are about 3% and 12% in exponential and stationary phase cells, respectively. Similarly to the wild type, the strain expressing the full length *ScLSM4* gene shows about 1% and 3.5% of cells with fragmented nuclei in exponential and stationary phase, confirming that this feature is dependent on the expression of the truncated form of the *LSM4* gene, as already demonstrated for its *K. lactis* counterpart.

To evaluate the ROS production and accumulation, the percentage of ROS positive cells were detected using the DHR-123 staining. During the exponential phase, about 2% and 12% of cells for the wild type and the *Sclsm4Δ1* mutant cells and about 4.7% in the *ScLSM4* expressing strain show positivity to the dye. As the cell's growth progresses, the percentage of ROS positive cells increases and during stationary phase it reaches 60% in the *Sclsm4Δ1* strain, about six time more than the wild type and the *ScLSM4* expressing strain (Figure 6, panels C and D), confirming what we previously demonstrated for the *Kllsm4Δ1* mutant. The higher ROS accumulation of the mutant during senescence could rely on the abnormal accumulation of mRNAs in the cytoplasm, that can be easily oxidated and in turn promotes the premature entry in the regulated cell death program.

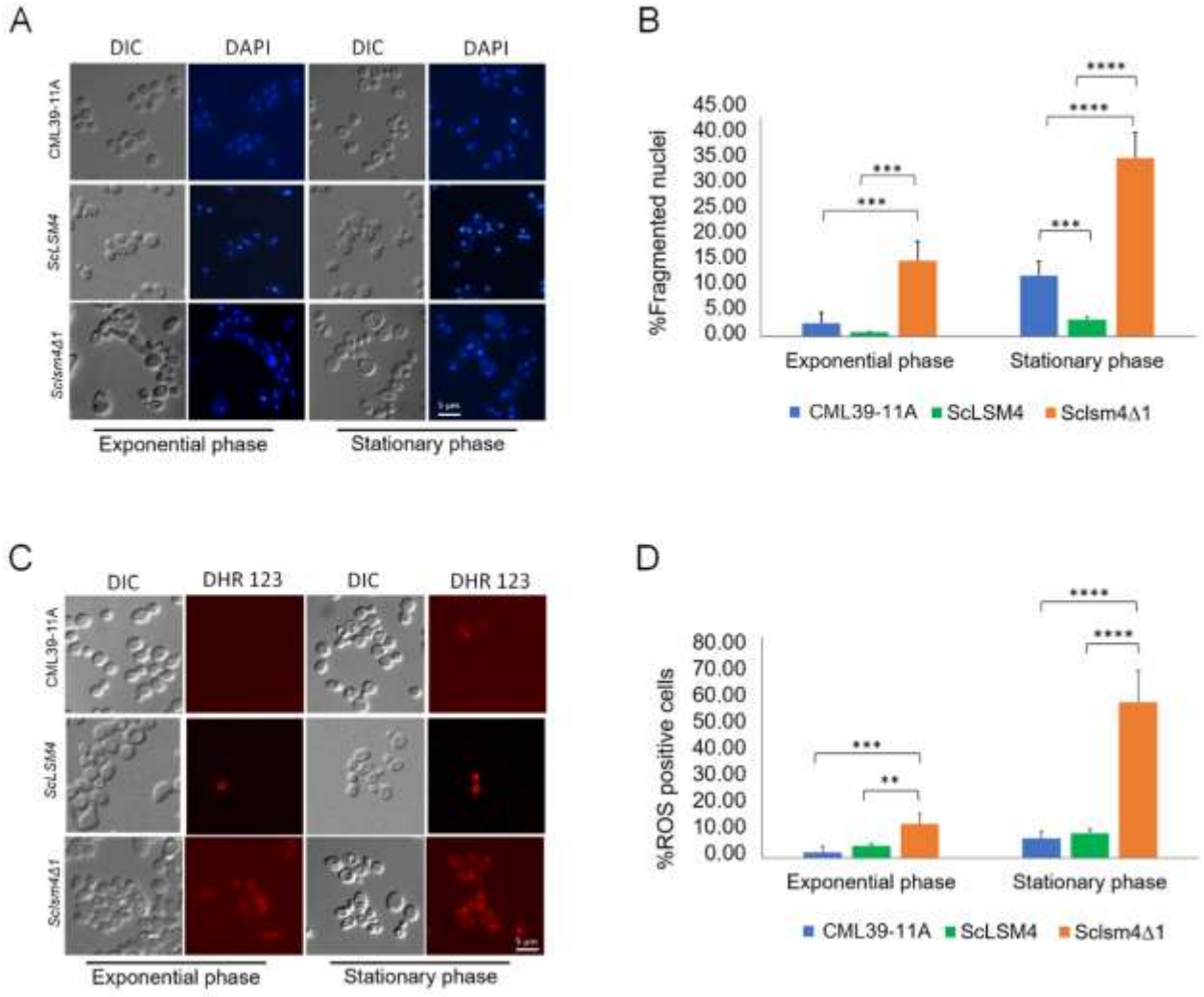

Figure 6. (A) DAPI staining of the CML39-11A (wild type), MCY4/*Sclsm4Δ1* mutant cells and MCY4/*ScLSM4* in both exponential and stationary phase, quantification of the percentage of fragmented nuclei over total cells from three independent experiments is plotted in **(B)**. **(C)** Dihydrorhodamine 123 (DHR-123) staining of the CML39-11A (wild type) and MCY4/*Sclsm4Δ1* mutant cells and MCY4/*ScLSM4* in both exponential and stationary phase, quantification of the percentage of ROS positive cells over total cells from three independent experiments is plotted in **(D)**. Data are represented as mean percentage of 700 cells per set ± standard deviation. ***p-value<0.001, ****p-value<0.0001

Finally, we tested the growth of the *Sclsm4Δ1* mutant strain on complete medium (YPD) added with different compounds known to increase the oxidative stress, in the case of the acetic acid 60 mM, or whose sensitivity is linked to autophagy defects, such as caffeine at a concentration of 0.25% (Kumar *et al.*, 2019). The mutant shows high sensitivity to both compounds, and also lower growth on complete medium in which the carbon source is glycerol (Figure 7, panel A), as reported for *Kllsm4Δ1* (Mazzoni *et al.*, 2005). These phenotypes are easily restored by the expression of the full-length *LSM4* gene, as seen in the *ScLSM4* strain, especially referred to

caffeine and acetic acid exposure. The growth on glycerol, on the other hand, is only partially restored when compared to the wild type, suggesting an intrinsic defect of growth of the MCY4 strain on non-fermentable carbon sources. Similar sensitivity is shown also in a mutant lacking the *LSM1* gene (*lsm1Δ*), which is a component exclusively of the cytoplasmic LSM complex, strengthening the hypothesis that LSM defects could lead to misfunctioning stress response (Figure 7, panel B). The differences in genetic background between the BMA38 strains and the CML39-11A and MCY4 strains, result in different sensitivity to the stress compounds, therefore to highlight the differences between the wild type (BMA38) and the mutant strain (BMA38 *lsm1Δ)* we had to use a lower concentration (0.15%) of caffeine, as the BMA38 genetic background resulted more sensitive to this compound compared to CML39-11A and MCY4 strains.

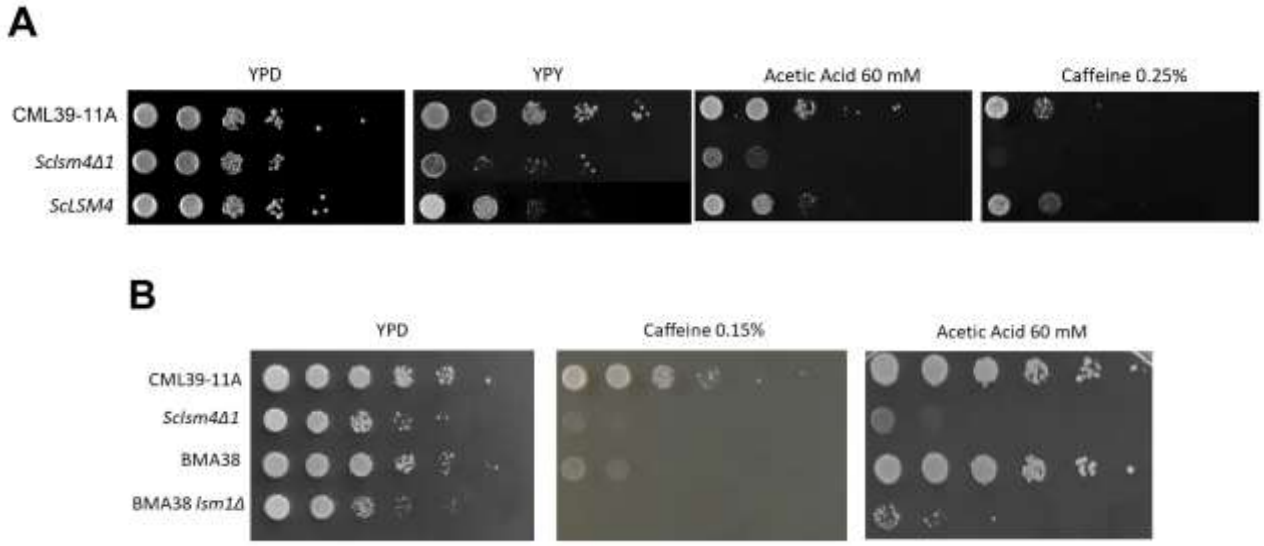

Figure 7. (A) 10-fold dilution of exponential growing cultures in YPD of CML39-11A (wild type), MCY4/ *Sclsm4Δ1* mutant cells and MCY4/*ScLSM4* were spotted on complete solid media containing 2% glycerol (YPY), YPD containing 60 mM acetic acid and 0.25% caffeine and plates were incubated at 28°C for 3 days. YPD was used as growth control. **(B)** Caffeine and acetic acid sensitivity test of MCY4/*Sclsm4Δ1* and *lsm1Δ* and their wild types (CML39-11A and BMA38). 10-fold dilutions were spotted on YPD plates supplemented with caffeine 0.15% and acetic acid 60 mM and incubated at 28°C for two days. YPD plates were used as growth control.

5.2 The use of low doses of rapamycin does not protect both wild type and mutant cells from oxidative stress

The oxidative stress can trigger autophagy both in yeast and in mammalian cells (Lei *et al.*, 2022), while a recent study reported that the use of a well-known autophagy inducer like rapamycin, can improve the neuroprotection against ageing-induced oxidative stress in aged rats (Singh *et al.*,

2019). As demonstrated for *Kllsm4Δ1* mutant strain (Mazzoni *et al.*, 2005), the *Sclsm4Δ1* mutant strain rapidly loses viability when treated with increasing concentration of hydrogen peroxide (H_2O_2), while the expression of the full-length *LSM4* gene restores the sensitivity to a wild type level (Figure 8). Then we tested the response of the mutant cells to the drug rapamycin. Accordingly to the impaired growth on the autophagy inducing medium, such as the YPD with caffeine 0.25%, the *Sclsm4Δ1* mutant strain resulted highly sensitive to low doses of rapamycin during the exponential phase, as the viability dropped to 4% within 4 hours of treatment with 6 nM rapamycin, while in the wild type the viability remained equal to the untreated cells (Figure 9, panel A). Similar results were obtained testing the sensitivity to the drug of a yeast mutant for another component of the LSM complex, the *lsm1Δ* mutant strain, which is part of the cytoplasmic Lsm1-7 complex needed for the correct association with the decapping machinery (Mayes *et al.*, 1999). Both *Sclsm4Δ1* and *lsm1Δ* mutant strains with their respective wild types (CML39-11A and BMA38) were spotted in serial dilutions on YPD plates containing rapamycin 6 nM, and the impairment of growth that is seen in Figure 9, panel B, demonstrated the high sensitivity to the drug also for the *lsm1Δ* mutant, suggesting that in both *LSM* mutants the autophagic process is impaired. Again, the differences in sensitivity between the two wild types (CML39-11A and BMA38) observed in Figure 9, panel B are probably due to the different genetic background of the strains.

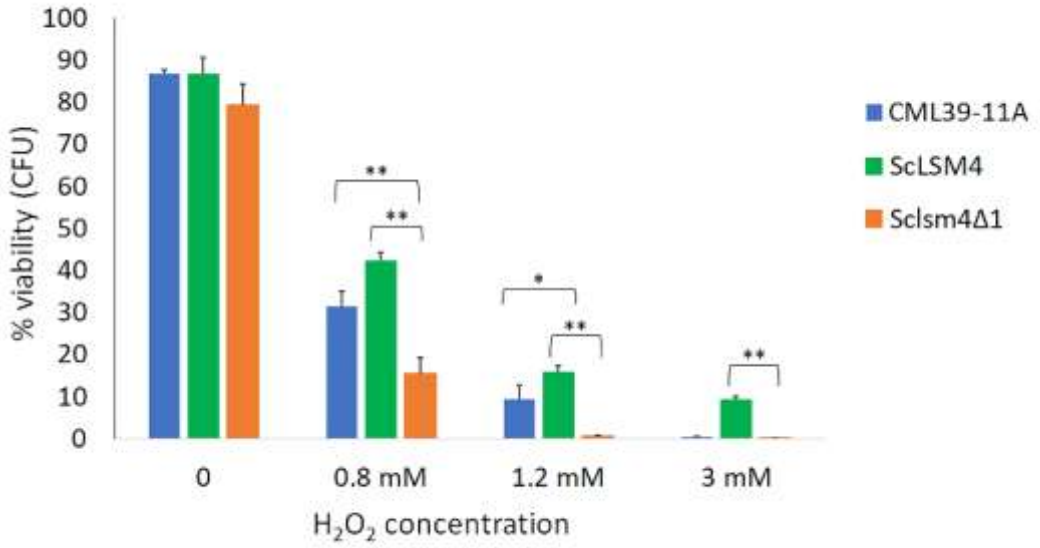

Figure 8. Oxidative stress test performed on strains CML39-11A (wild type), MCY4 expressing *Sclsm4Δ1* mutant or the full length LSM4 protein (*ScLSM4*) cells. Cell viability was measured after exposure to H_2O_2 at the indicated concentrations for 4 hours. *p-value<0.05 **p-value<0.01

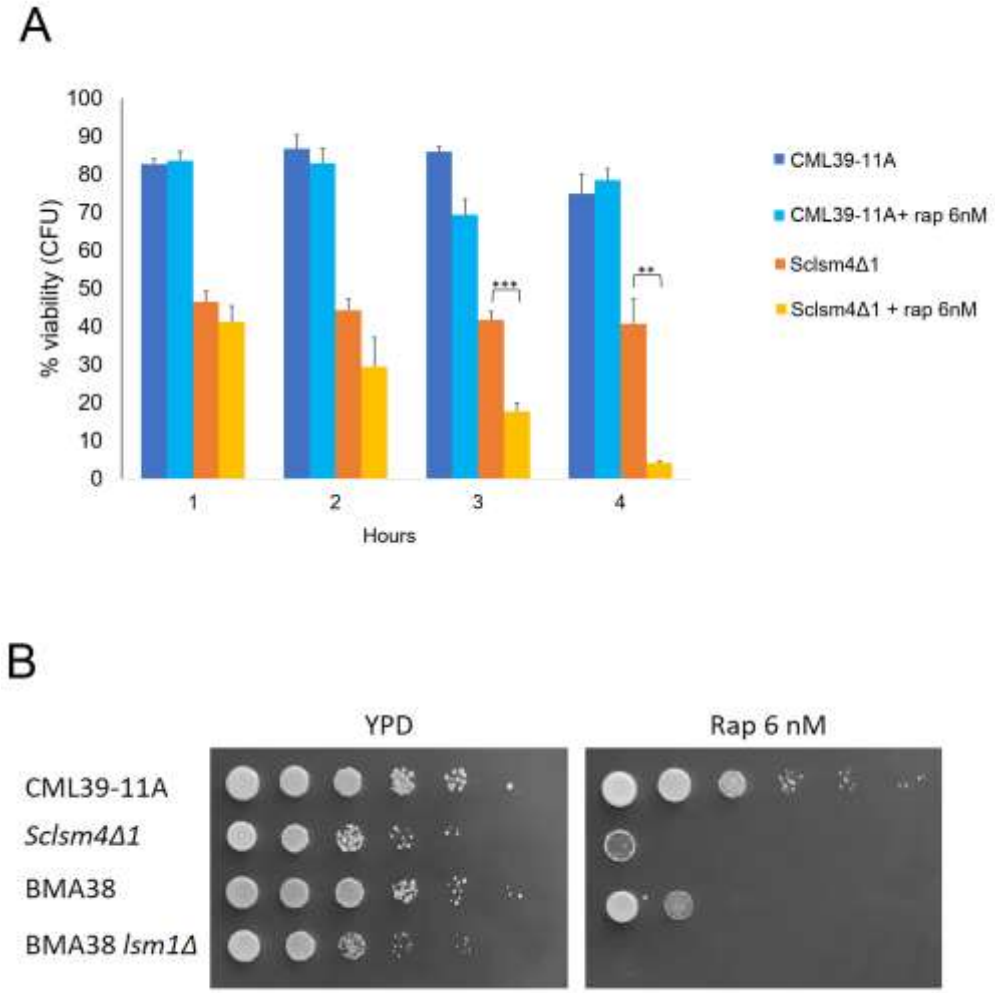

Figure 9. Rapamycin treatment of the strains of interest. **(A)** Cell viability of the CML39-11A (wild type) and MCY4 expressing *Sclsm4Δ1* was measured every hour after 4 hours treatment with 6 nM of rapamycin in SD medium. **(B)** 10-fold dilutions of *Sclsm4Δ1* and *lsm1Δ* and their wild type strains (CML39-11A and BMA38, respectively) were spotted on YPD plates supplemented with rapamycin 6 nM and incubated at 28°C for two days. YPD plates were used as growth control. Data are represented as the mean of three independent experiments ± standard deviation. **p-value<0.01 ***p-value<0.001.

Then we tested if the same amount of rapamycin could protect cells from hydrogen peroxide induced cell death, as a recent study demonstrated that rapamycin-induced autophagy could protect old rats brains from ageing-induced oxidative stress (Singh *et al.*, 2019). In the wild type cells, the presence of 6 nM rapamycin did not protect them from oxidative stress, as the differences in viability of the treated and untreated samples after additional 4 hour of exposure to different concentration of H_2O_2 after 4 hours of rapamycin treatment were not statistically significant. On the other hand, it was not possible to evaluate the protective action of rapamycin in the *Sclsm4Δ1* mutant due to its high toxic effect (Figure 10). Similar results with no statistical significance in terms of rapamycin-induced protection were obtained using even lower doses of H_2O_2 to mimic the

ageing-related oxidative stress as described in (Poljak *et al.*, 2003), therefore confirming that the low dose of rapamycin used in this work is not sufficient to protect the tested strains from a wide range of oxidative stress (Figure 11, Supplemental Figure 1).

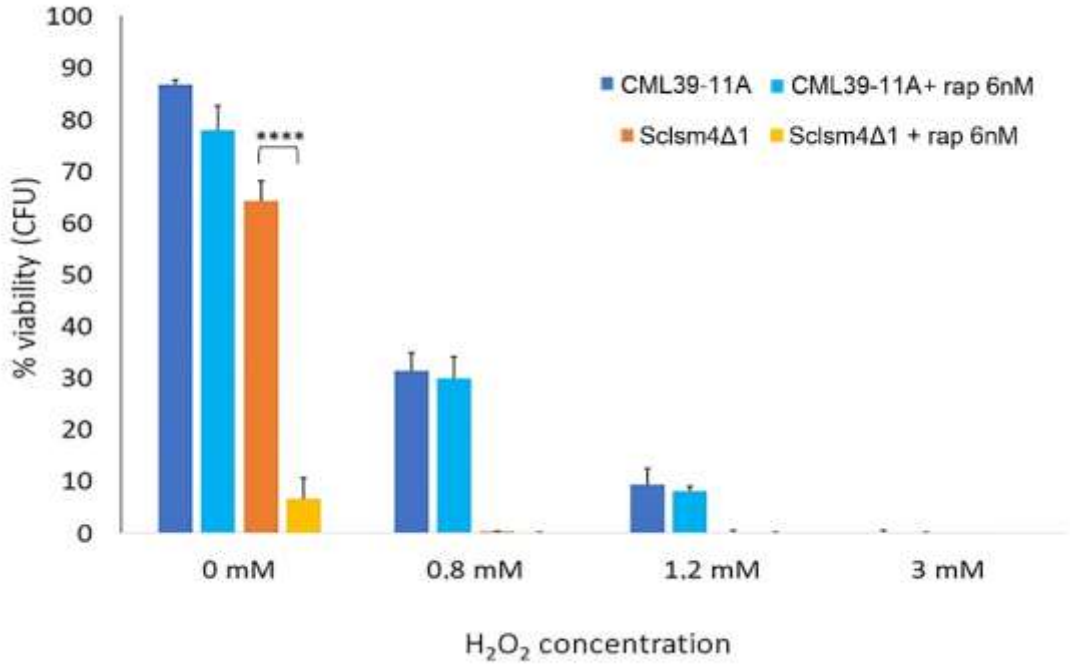

Figure 10. Cell viability of the CML39-11A (wild type) and *Sclsm4Δ1* mutant was measured after exposure to H_2O_2 at the indicated concentrations for 4 hours. 4 hours treatment with rapamycin 6 nM was performed prior to the exposure to H_2O_2. Data are represented as the mean of three independent experiments ± standard deviation. ****p-value<0.0001

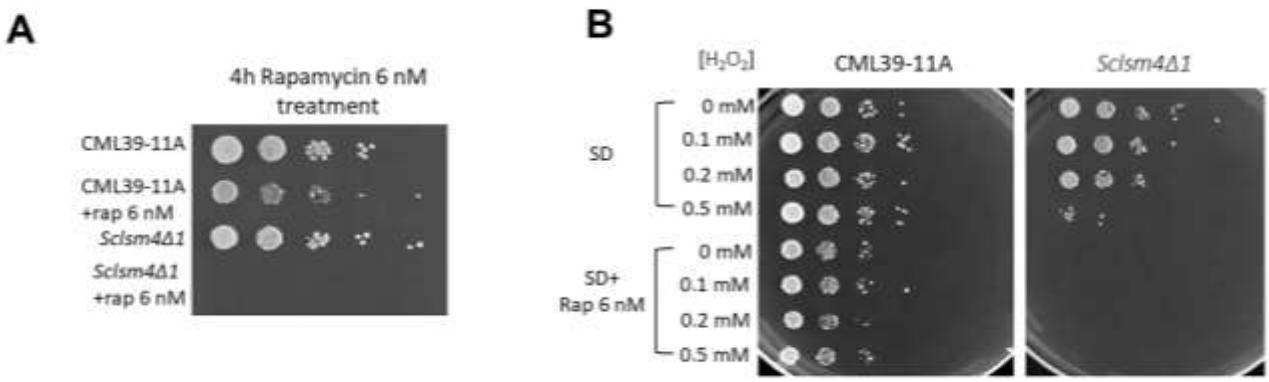

Figure 11. Cell viability of the CML39-11A (wild type) and *Sclsm4Δ1* mutant was measured after exposure to H_2O_2 at the indicated concentrations for 4 h. 6nM rapamycin was added 4h prior exposure to H_2O_2. **(A)** 10-fold dilution were spotted on complete solid media YPD after 4 hours of incubation in SD and SD + rapamycin 6 nM, and plates were incubated at 28°C for 3 days. **(B)** Treated and untreated samples with rapamycin 6 nM were spotted in 10-fold dilution on complete solid media YPD after 4 hours of incubation with low doses of H_2O_2 as described in (Poljak *et al.*, 2003), and plates were incubated at 28°C for 3 days.

5.3 Western blot analysis shows autophagy defects in the *Sclsm4Δ1* mutant strain

Taken together the forementioned experiments and the previous knowledge on the over-expression of *NEM1* that can suppress most of the phenotypes and oxidative sensitivity of the *Kllsm4Δ1* mutant strain (Palermo *et al.*, 2015), we monitored the autophagy flux in the *Sclsm4Δ1* mutant cells through the GFP-Atg8 processing assay (Daniel J. Klionsky *et al.*, 2021). The wild type and *Sclsm4Δ1* mutant strains were transformed with the pUG36/ATG8 plasmid, in order to synthesise the chimerical protein GFP-Atg8. The Atg8 protein is an autophagic marker, as it associates with the autophagosome membrane, and it is transported together with the cargo to the vacuolar compartment. The GFP β-barrel structure is more resistant than Atg8 to vacuolar hydrolysis, therefore the presence of free GFP on western blot indicates that the autophagic process has properly occurred and the autophagosomes have reached the vacuole. The nitrogen deprivation is known to highly and rapidly induce the autophagic process (Takeshige *et al.*, 1992; Cebollero and Reggiori, 2009), hence is usually employed to verify the correct functionality of autophagy. The autophagic flux has been evaluated also during the post-diauxic growth phase and in glucose-depleted medium, as the change in carbon source availability can also trigger the autophagic process (Iwama and Ohsumi, 2019). To exclude the possibility that a misregulation in the autophagy pathway and in the aminoacids recycle could lead to an improper activation of the *MET17* promoter on the pUG36/ATG8 plasmid, affecting the GFP-Atg8 processing assay itself, cells were grown on SD medium supplemented with auxotrophic requirements with the addition of methionine prior to the nitrogen and glucose starvation.

As we can see in Figure 12, the autophagy process is induced in the wild type strain (CML39-11A) after 16 hours of culture in synthetic medium (SD 2% glucose, lane 2, PD), in the nitrogen starvation condition (lane 3, SD-N) and in glucose starvation (lane 4, -glu), where it reaches 6.34%, 9.6% and 3.47% of activation, respectively. The results are very different in the mutant *Sclsm4Δ1*, as the percentage of autophagy activation is below 3% in the post-diauxic phase of culture in 2% glucose medium (lane 6, PD), while in nitrogen and glucose starvation the activation of the process is below 1% (lanes 7 and 8, SD-N; -glu), suggesting again a defect in the functioning of the autophagic process in the mutant. Due to high variability in the autophagy activation in the wild type in S-glu condition in all carried experiments, it resulted not statistically significant the difference with the mutant strain in this condition. Interestingly, the fusion protein GFP-Atg8

accumulates at higher level in the mutant in all the tested conditions, suggesting a stabilization at mRNA or protein level that need to be investigated in the future.

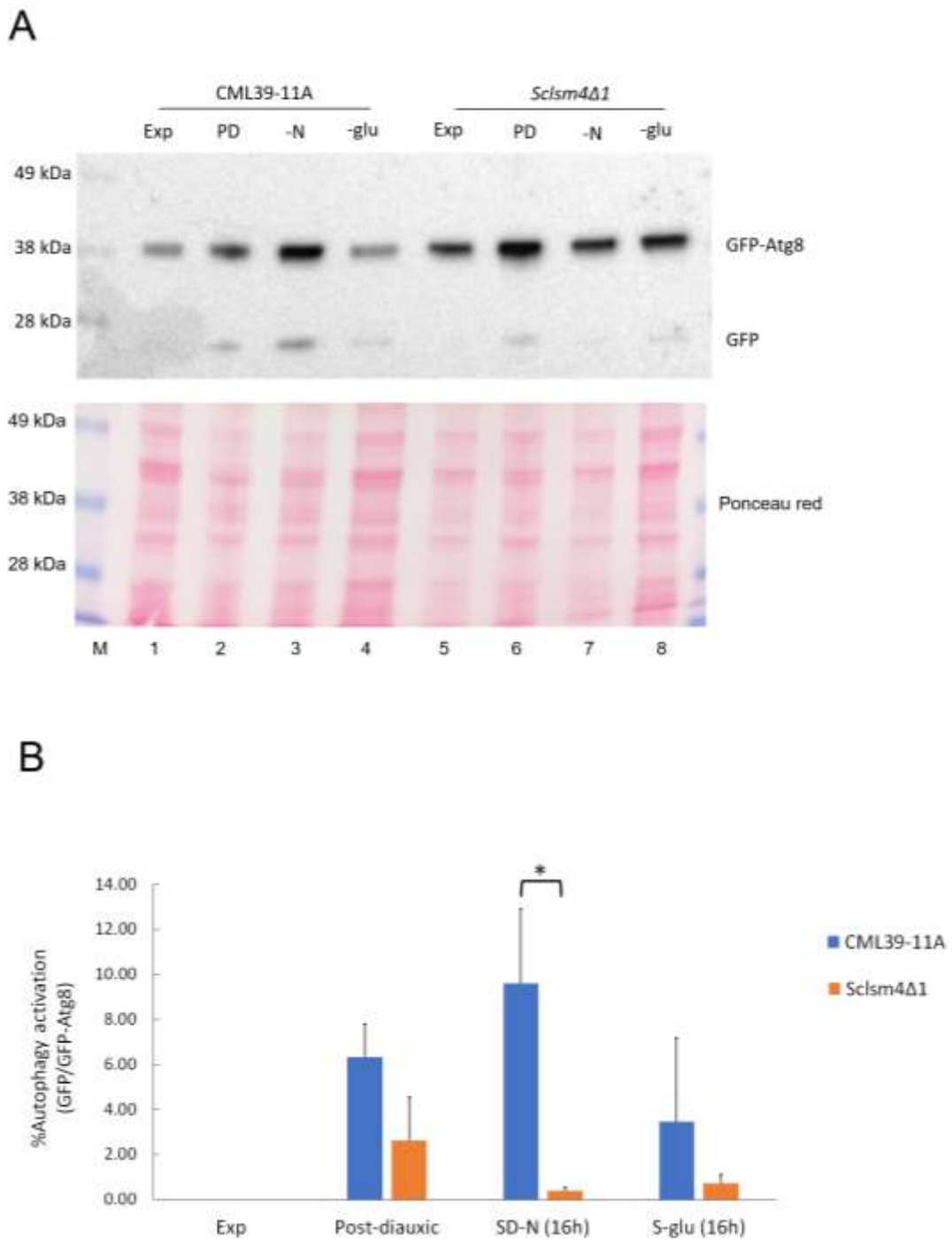

Figure 12. *Sclsm4Δ1* mutant shows defects in autophagy induction. **(A)** CML39-11A (wild type) and mutant *Sclsm4Δ1* cells were grown exponentially in SD medium (Exp), then the same amount of cells was centrifuged, washed and resuspended in SD, SD-N (nitrogen deprivation, -N) and S-glu (glucose deprivation, -glu) media and further incubated for 16 hours (PD: Post-diauxic phase). Ponceau red staining has been used as a load control. One of three independent

experiments is shown. **(B)** Percentage of autophagy activation was measured as the ratio between free GFP/GFP-Atg8 in three independent experiments, and data are represented as the mean and standard deviation. *p-value<0.05.

5.4 The *Sclsm4Δ1* mutant strain lifespan differs under nitrogen or glucose starvation

The calorie restriction plays a well-established role in regulating the TORC1 kinase activity, and in yeast the link between starvation and the extension of lifespan is well known (Fabrizio and Longo, 2003; Goldberg *et al.*, 2009). On the other hand, the nitrogen starvation is able to powerfully trigger the autophagy and mediates the clearance of damaged intracellular structures that in turn promotes the survival of the cells in wild type strains, while it has a detrimental effect on mutant strains unable to properly activate the autophagic process (Onodera and Ohsumi, 2005; Suzuki, Onodera and Ohsumi, 2011). Therefore we evaluated the Chronological Life Span (CLS) of the *Sclsm4Δ1* mutant strain and the wild type CML39-11A during different starvation conditions. As shown in Figure 13, panel A, the maintenance of the cells in a medium lacking the nitrogen source (SD-N) increased CLS in the wild type strain. On the contrary, MCY4 expressing *Sclsm4Δ1* cells in the same SD-N medium showed a drop in viability already after 1 day and completely lost viability one day before cells maintained in SD, at day 4.

Then we tested the viability of the strains during CLS in three types of culture media: SD containing 2% glucose (used as control), SD containing 0.1% glucose, representing the calorie restriction condition, and water, lacking any source of carbon and nitrogen, representing the extreme calorie restriction condition. The viability assay shows that the strains maintained in 2% glucose follow the previously characterised lifespan, with total loss of viability on day 9 and day 15 for *Sclsm4Δ1* and CML39-11A, respectively. Interestingly, under calorie and extreme calorie restriction, the lifespan highly increases, both in the mutant and the wild type (Figure 13, panels B and C). We found that the greater effect on lifespan and viability was under calorie restriction (glucose concentration at 0.1%), in which both strains maintained the ability to form microcolonies and high percentage of viability (above 10%) even after 28 days. This result is especially relevant for the mutant *Sclsm4Δ1*, in which the physiological lifespan is nearly half of the lifespan of the wild type. In fact, pinpointed day 27 as a checkpoint, the calorie restriction increases the mutant lifespan by 3-fold, while in the wildtype it represents only a 2-fold increase.

The different behaviour under nitrogen and energy starvation suggests a different regulation of the autophagic pathway, that will be discussed in the Discussion section.

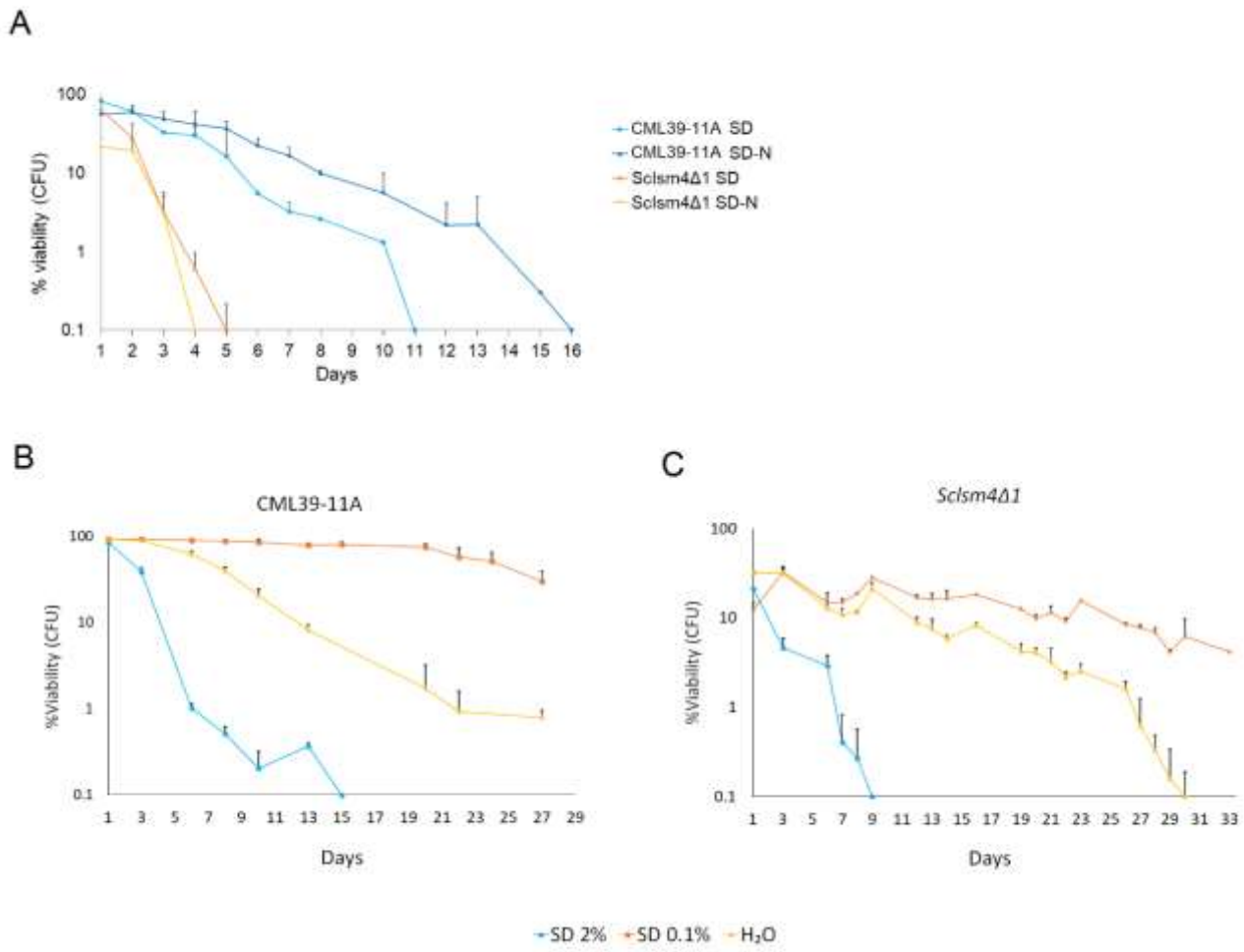

Figure 13. Chronological life span (CLS) of wild type (CML39-11A) and *Sclsm4Δ1* mutant strain in different nutrient conditions. **(A)** Cells cultured in nitrogen deprived medium (SD-N). CLS of wild type **(B)** and *Sclsm4Δ1* **(C)** cells cultured in calorie restriction medium (SD with glucose 0.1%) and extreme calorie restriction (water). Synthetic defined medium (SD) was used as control. Data are represented as the mean and standard deviation of three independent experiments.

5.5 The *Sclsm4Δ1* mutant strain accumulates autophagic structures in the cytoplasm

The autophagic process implies the formation of a double-membrane structure which expands in the cytoplasm forming a sealed vesicle around the cargo, known as autophagosome (AP). The transport and fusion of the AP to the vacuole leads to the degradation and recycling of the sequestered material, such as damaged proteins, bulk RNAs which failed to be degraded by specialised exonucleases, and entire portions of organelles. Therefore, the autophagic flux can be monitored by the localization of the Atg8 protein, which is resident in the autophagosome membrane from the nucleation and expansion to the fusion with the vacuole (Kirisako *et al.*, 1999; Obara *et al.*, 2008). The expression of the chimerical protein GFP-Atg8 in the strains of interest

allowed us to follow the autophagosome localization at different growth phases and in different media by fluorescent microscopy.

Initially, during exponential phase of growth in SD medium, around 1% and 7% of the wild type and *Sclsm4Δ1* mutant cells, respectively, showed a single GFP-Atg8 dot, suggesting the proximity of early autophagosome to the vacuole membrane (Figure 14, panel A, SD exp), while most of the fluorescence was uniformly distributed into the cytoplasm. During this growth phase, a small percentage of *Sclsm4Δ1* mutant cells showed two or more GFP-Atg8 dots per cell. When the cells were cultured under nitrogen starvation condition (SD-N) for 4 hours, the differences between the wild type and the mutant increased, with a mean percentage of GFP-Atg8 dots around 3% for the wild type and 25% for the *Sclsm4Δ1* mutant (Figure 14, panel A, SD-N 4h). Moreover, also the number of cells showing ≥2 GFP-Atg8 dots increased in the mutant strain to about 12%, representing half of cell population with GFP-Atg8 dots. As the time in nitrogen starvation increased, the wild type cells showed most of the fluorescence in the vacuole, confirming the active autophagic flux, with only a slight increase of cells showing cytoplasmic dots (Figure 14, panel C, SD-N 16h), while about 35% of *Sclsm4Δ1* mutant cells showed cytoplasmic dots and half of them presented 2 or more dots per cell and very low intravacuolar fluorescence.

During the stationary phase in SD medium (three days of culture) more than 90% of *Sclsm4Δ1* mutant cells resulted positive to cytoplasmic GFP-Atg8 dots, while in the wild type cells resulted positive about 13% of the population (Figure 14, panel E). This percentages increases a little bit in the wild type incubated for 3 days in SD-N medium, while interestingly in the *Sclsm4Δ1* mutant cells those presenting GFP-Atg8 dots after 3 days in SD-N medium were the same as after 16h of incubation in SD-N (about 40%), suggesting a stabilization of these structures in opposition to their physiological disappearance over time (Geng *et al.*, 2008). This could also be due to the rapid loss of viability of the *Sclsm4Δ1* mutant in SD-N observed already at day 1 (Figure 13, panel A). These data altogether, indicate that *Sclsm4Δ1* mutant cells accumulates autophagy-related structures when autophagy is induced by nitrogen starvation or during ageing, and further vacuolar co-localization analysis are planned to confirm this evidence.

The same analysis was performed with the *lsm1Δ* mutant in a different genetic background with similar results (Figure 15), suggesting that the observed autophagy defects are a feature of *LSM* mutants. Interestingly, one of the differences between the *lsm1Δ* mutant and the *Sclsm4Δ1* mutant is an overall lower percentage of cells with GFP-Atg8 dots, in particular in the stationary phase both in SD and SD-N medium, but with a higher presence of two or more dots per cell. Furthermore, the correspondent wild type (BMA38) showed a slightly lower percentage of cells with GFP-Atg8 dots compared to the wild type CML39-11A, especially in SD-N after 16h of incubation, suggesting a difference in autophagosome formation or transport dependent on the genetic background.

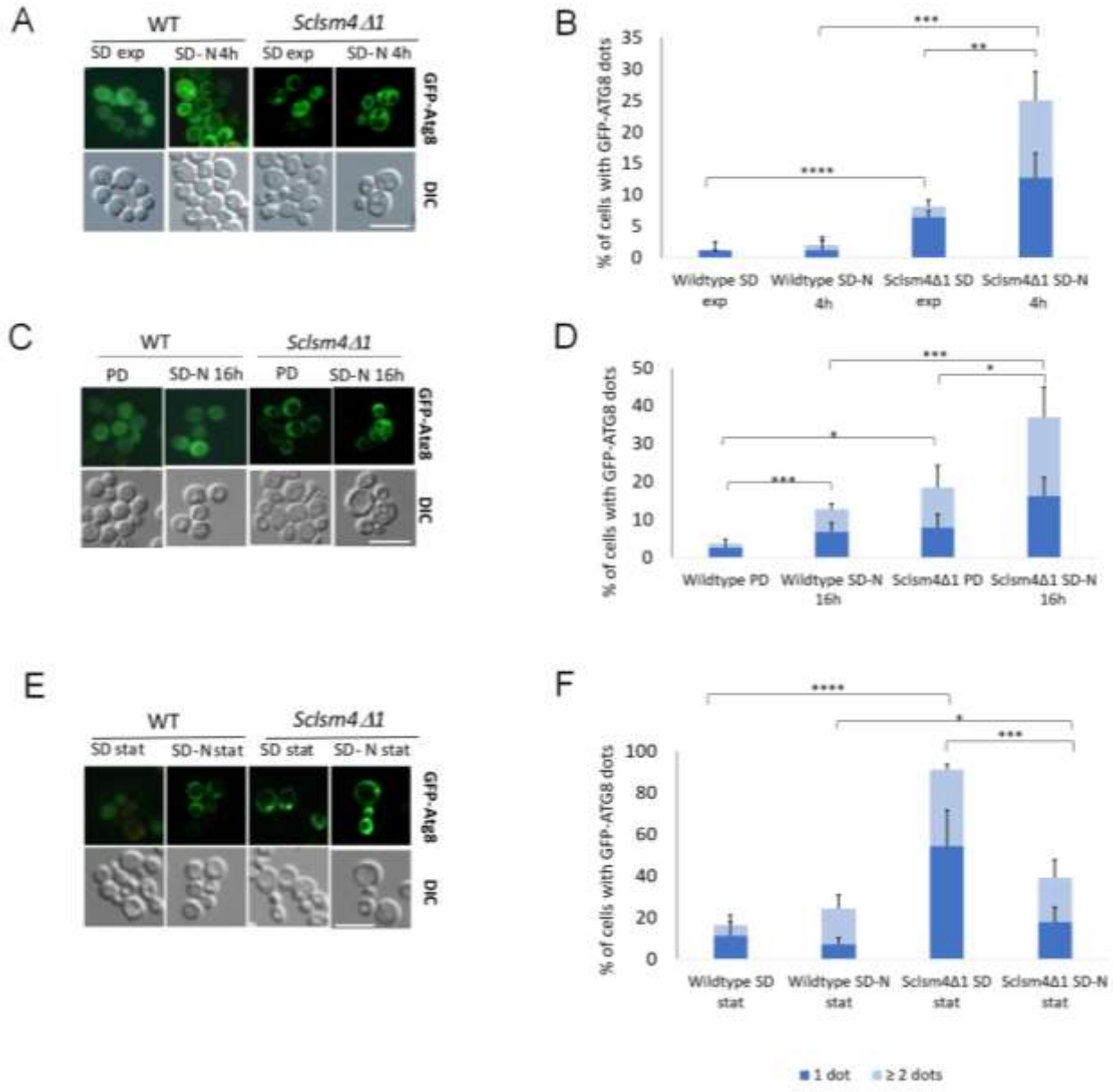

Figure 14. Wild type CML39-11A and MCY4/*Sclsm4Δ1* cells expressing the fusion protein GFP-Atg8 were observed at the fluorescent microscope during exponential phase in both SD and SD-N medium for 4h **(A)**, during post diauxic phase (PD) and in SD-N for 16h **(C)** and after 3 days of growth in SD (SD stat) or SD-N (SD-N stat) **(E)**. GFP-Atg8 dots per cell were quantified from three biological replicates (n ≥ 300 cells), and the mean of cells containing one or ≥2 dots is plotted in **(B)**, **(D)** and **(F)**. Scale bar: 5 μm. Error bars represent standard deviation. *p-value<0.05 **p-value<0.01 ***p-value<0.001 ****p-value<0.0001.

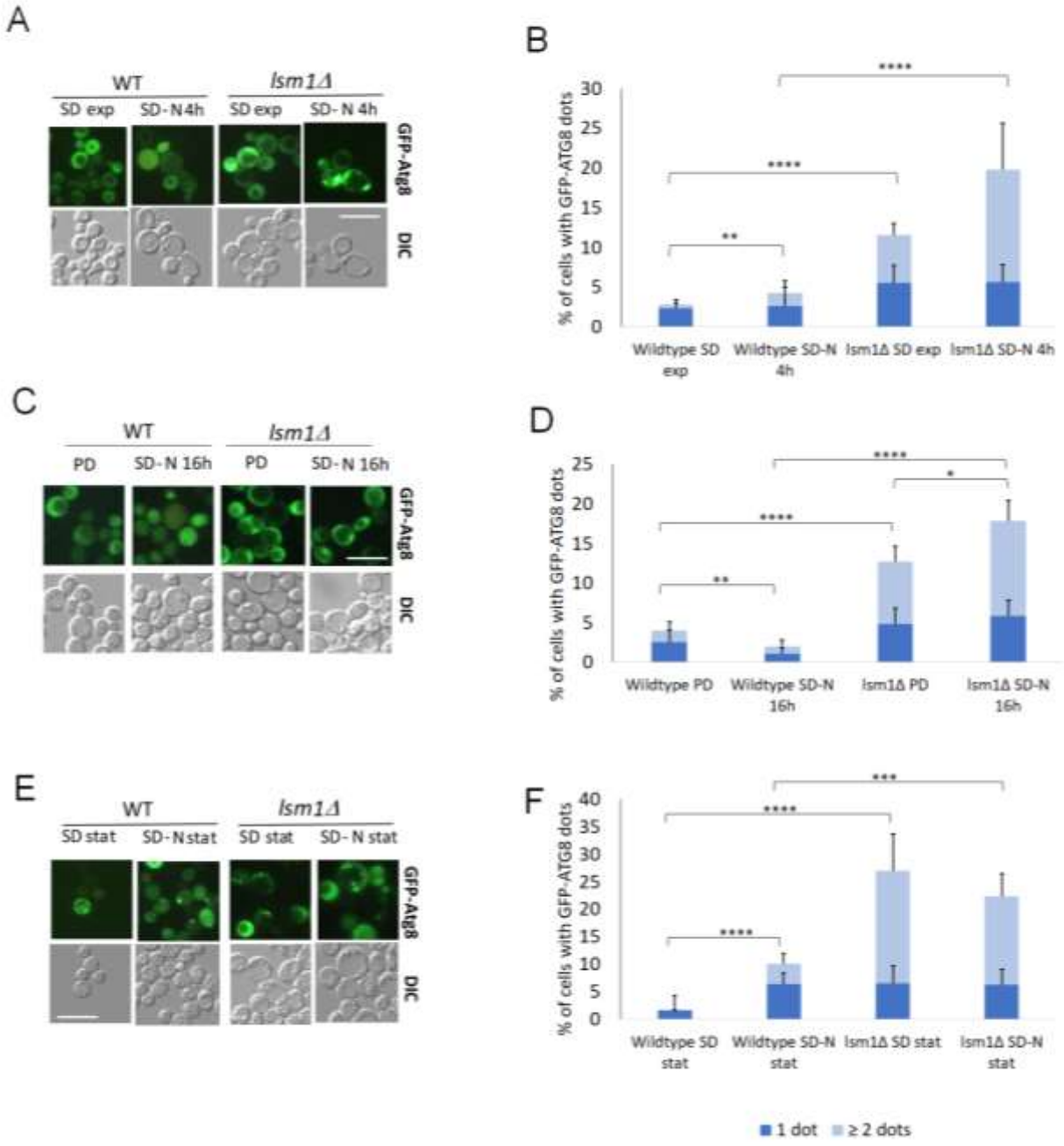

Figure 15. Wild type BMA38 and *lsm1Δ* cells expressing the fusion protein GFP-Atg8 were observed at the fluorescent microscope during exponential phase in both SD and SD-N medium for 4h **(A)**, during post diauxic phase (PD) and in SD-N for 16h **(C)** and after 3 days of growth in SD (SD stat) or SD-N (SD-N stat) **(E)**. GFP-Atg8 dots per cell were quantified from three biological replicates (n ≥ 300 cells), and the mean of cells containing one or ≥2 dots is plotted in **(B)**, **(D)** and **(F)**. Scale bar: 5 μm. Error bars represent standard deviation. *p-value<0.05 **p-value<0.01 ***p-value<0.001 ****p-value<0.0001.

5.6 The *Sclsm4Δ1* mutant strain shows later autophagy activation during ageing in extreme calorie restriction

To better understand the underlying causes of the increased life span during calorie restriction, and asses if the autophagy pathway could be involved, we analysed the autophagy activation after three and four days of culture in the media described before, SD 2% glucose, SD 0.1% glucose and water. We additionally tested the activation of autophagy also in PBS (phosphate buffered saline) cultured cells to ensure the ideal osmolarity of the medium without adding any carbon or nitrogen source. What we found is that during ageing the autophagy is early activated in the extreme calorie restriction condition (water and PBS) in the wild type strain already on day 3, while in the mutant we see a band corresponding to the cleaved fusion protein only after four days of culture in water (Figure 16). Moreover, the percentage of activation of the autophagic process is lower in the *Sclsm4Δ1* strain compared to the wild type. In addition, we did not report any activation of the process in calorie restriction condition, represented by the SD medium with 0.1% glucose, despite its strong positive effect on the viability of both strain (Figure 13). Again, these results reinforced our hypothesis on the different regulation of the autophagy pathway under nitrogen and aminoacids starvation versus glucose and energy deprivation, suggesting that the mutation in the *LSM4* gene could impair only a subset of branches of the autophagic pathway.

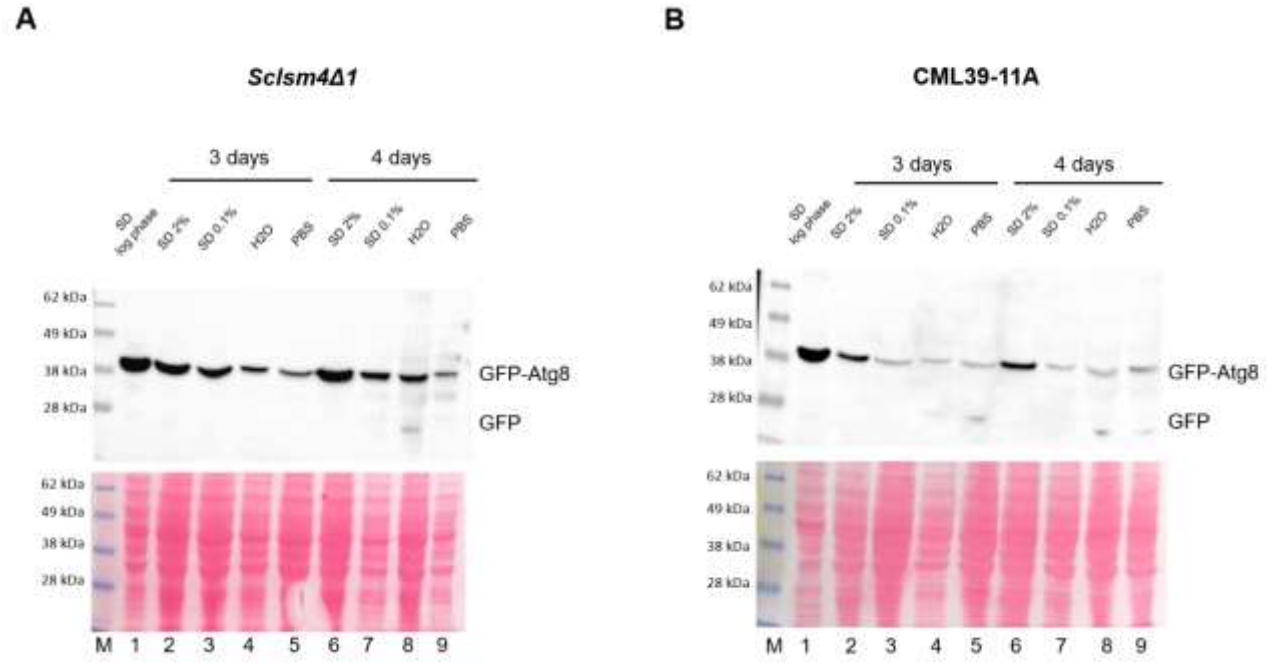

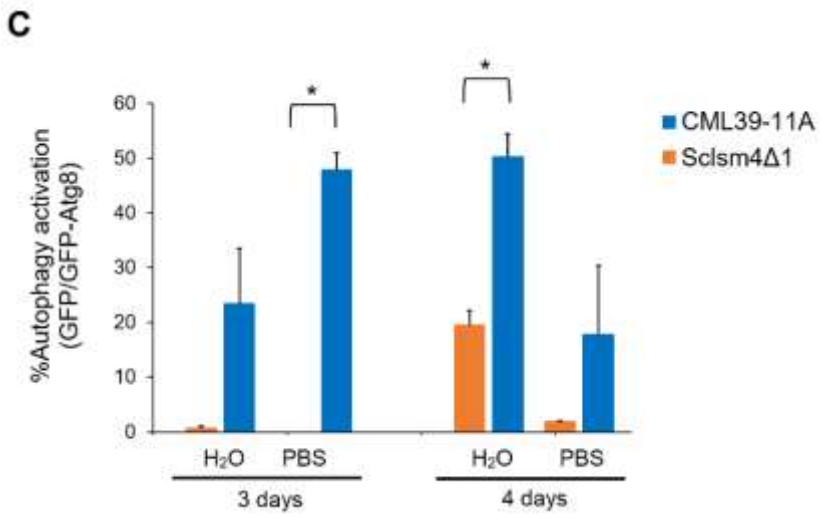

Figure 16. Western Blot analysis on **(A)** mutant (*Sclsm4Δ1)* and **(B)** wild type (CML39-11A) cells expressing the fusion protein GFP-Atg8 cultured in different media (SD, SD 0.1% glucose, water and PBS) for 3 days and 4 days. One of two independent experiments is shown. Ponceau S staining was used as loading control**. (C)** Percentage of autophagy activation was measured as the ratio between free GFP/GFP-Atg8 in two independent experiments, and data are represented as the mean and standard deviation. *p-value<0.05.

5.7 The *Sclsm4Δ1* mutant strain shows high levels of extracellular RNAs and large extracellular structures during ageing

The main characteristic of the *Sclsm4Δ1* mutant is the abnormal accumulation of RNAs in the cytoplasm, which increases the sensitiveness to oxidative stress and causes the premature ageing and the early onset of regulated cell death markers. Therefore, the increase of the life span described under calorie restriction could depend on a change in RNAs metabolism which could relief the cell from this type of stress and, as we have already explored, the autophagy is one of the possible processes involved. Another possibility for the cell to dispose of the RNAs bulk is the secretion in the extracellular environment, which can occur in a specific and regulated way or in a non-specific and accidental way.

In this regard, we analysed the nucleic acid content of the supernatant of our cultures in water after four days and we found that small or fragmented RNAs accumulate in the supernatant of *Sclsm4Δ1* strain, while there was not a visible band in the samples derived from SD cultured cells or derived from the wild type strain (Figure 17), and when treated with RNase the bands are no longer visible, confirming the nature of the nucleic acid (Supplemental Figure 2). Additionally, we

monitored the OD_{600} of the cultures and there was not a significant decrease in cellular mass, proving that the release of the nucleic acid was not due to cellular disruption.

The secretion of RNAs in the extracellular compartment could then represent a new crucial survival mechanism that need to be further explored. In fact, our future studies will concern if the RNAs are secreted through regulated mechanisms, such as extracellular vesicles, and if there is any specificity in the choice of the cargo and what species of RNAs are preferentially secreted.

Interestingly, as in day four of culture in water we can see the autophagy activation in the mutant cells (Figure 16), it would be of great interest to deepen the possible link between the secretion of RNAs and the autophagy induction.

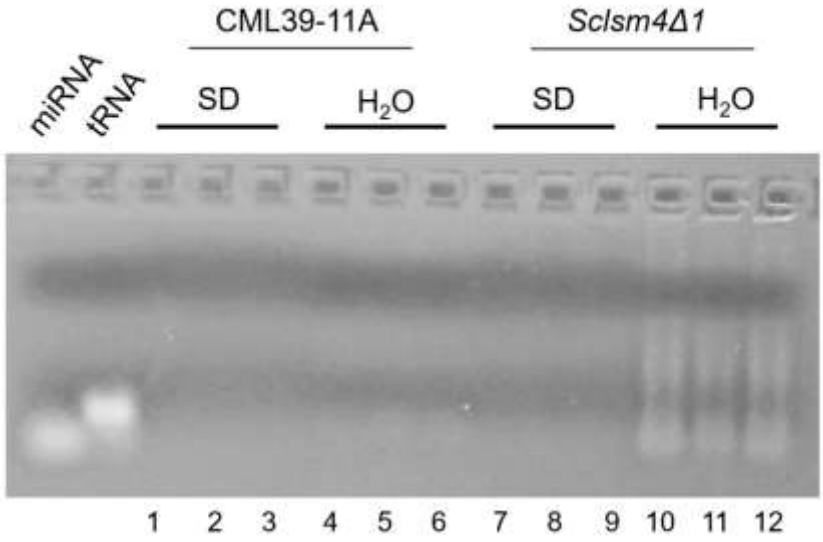

Figure 17. Electrophoresis analysis on agarose gel of supernatant RNAs after 4 days of culture in the described media. The secretion of small (<100 nt) or fragmented RNAs is more effective in extreme calorie restriction (water) in the mutant strain (*Sclsm4Δ1)* while it does not occur in the wild type strain (CML39-11A). A tRNA (90 nt) and a miRNA (20 nt) were used for size comparison. Three biological replicates are shown.

As a different approach, we analysed the nucleic acid content of the supernatant of the cells cultured on solid SD media, with the protocol described by (Reis *et al.*, 2019), in which they isolate extracellular vesicles from *C. neoformans* and *C. gattii* cultured on agar plates and resuspended in PBS. We did not perform the ultracentrifugation, instead we sequentially filtered the PBS medium in which we harvested the cells in order to investigate if there are any differences in RNA accumulation associated with different size of putative EVs. Interestingly, after three days of culture on SD plates, the *Sclsm4Δ1* strain showed a high accumulation of extracellular RNA, while it was not detectable in the samples harvested from the CML39-11A strain, as shown in Figure 18. Regarding the enrichment in RNA associated with different filtration size from the *Sclsm4Δ1* strain

cultured on solid SD media, we reported that the sample filtrated at 0.8 μm (lane 7) showed a little increase in enrichment compared to the non-filtered sample (lane 6), then the RNA concentration decreased dramatically in the samples filtrated at 0.45 μm (lane 8) and at 0.1 μm (lane 10), while in the sample filtrated at 0.22 μm (lane 9) we saw again an enrichment comparable to the one found in the 0.8 μm filtrated sample (Figure 18). As known from literature, the extracellular vesicles could vary in size and dimension based on their biogenesis, with exosomes being the smallest (30-100 nm in diameter) derived from the endosomal compartment, microvesicles derived from plasma membrane ranging from 100 to 1000 nm, and apoptotic bodies spanning from 50 to 5000 nm (Suchorska and Lach, 2015). Therefore, the selective enrichment of RNA that we reported suggests the presence of vesicles with a diameter <0.8 μm and <0.22 μm, and their effective size need to be further analysed to confirm dimension and origin.

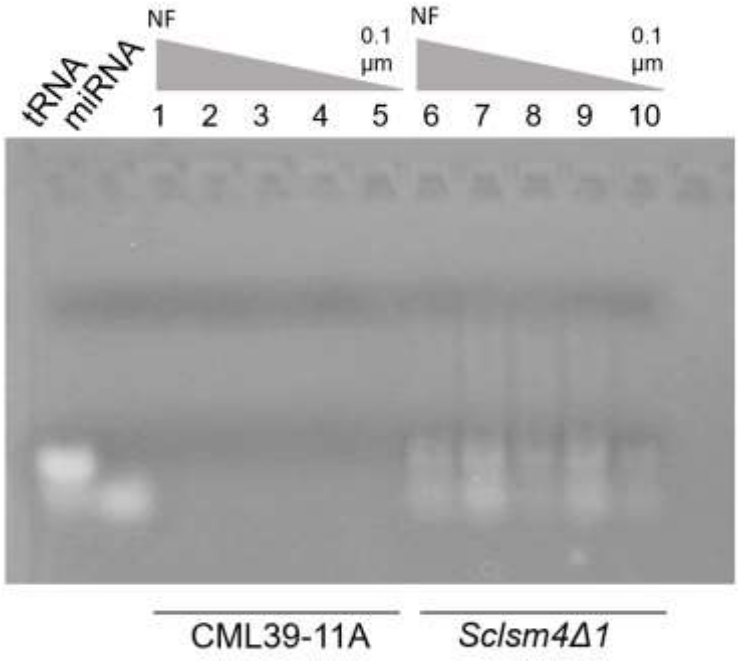

Figure 18. Electrophoresis analysis on agarose gel of RNAs extracted from PBS-resuspended cells, for the wild type strain CML39-11A (lanes 1-5) and *Sclsm4Δ1* mutant strain (lanes 6-10), after three days of growth on SD plates. The supernatant was filtered at 0.8 μm (lanes 2 and 7), 0.45 μm (lanes 3 and 8), 0.22 μm (lanes 4 and 9) and 0.1 μm (lanes 5 and 10). Lanes 1 and 6 represent the non-filtered samples. A tRNA (90 nt) and a miRNA (20 nt) were used for size comparison.

To further analyse if the RNA secreted in the supernatant could derived from a regulated vesicle trafficking, we inoculated the cells on a microscope slide coated with YPD medium and observed at the optic microscope after five days of growth at 28°C. Thanks to the agar medium, extracellular particles were trapped around the producing cells, allowing us to see them and preliminarily

analyse their size. Interestingly, the mutant cells seemed to produce larger and denser extracellular structures, which could represent apoptotic bodies (Figure 19).

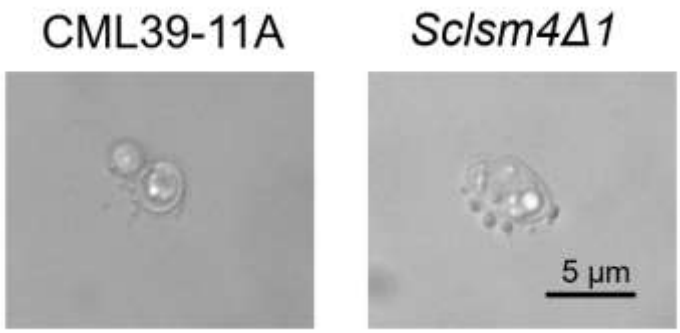

Figure 19. Micrography of wild type (CML39-11A) and mutant (*Sclsm4Δ1)* cells cultured for five days on a YPD coated slide, observed at the Axioskop 2, Carl Zeiss, Germany, microscope (100x). One representative field out of 10 is shown.

5.8 Construction of the *lsm4Δ1*-GFP genome mutant strain using the CRISPR/Cas9 editing system

Given the similarities in acetic acid, caffeine and rapamycin sensitivity (Figure 7 and Figure 9) and in the percentage of cells presenting autophagic structures in the cytoplasm (Figure 14 and 15) between the MCY4/*Sclsm4Δ1* and the *lsm1Δ* strains, it was of our interest to give rise to a mutant yeast strain in the *LSM4* gene in another genetic background to further confirm the link between *LSM* truncation and autophagy defects. Furthermore, yeast cells are easy to manipulate and there are plenty of expression vectors that can be used to create biotechnological strains, but the trans-gene expression and protein production could not represent the physiological scenario. Therefore, we choose to use the genome editing to overcome this problem, as the widely used editing system based on the *Streptococcus pyogenes* endonuclease Cas9 has been optimised also for yeast cells.

In this work, we used a system of two plasmids developed by Di Carlo et al. and optimised by Borodina and colleagues (DiCarlo *et al.*, 2013; Stovicek, Borodina and Forster, 2015), one carrying the Cas9 gene (pCfB2312) under the control of the relatively strong TEF1 promoter, the other (pCfB2311) carrying the gRNA molecule under the control of the SNR52 promoter, specific for RNA polymerase III binding, to prevent post-transcriptional RNA modification added by RNA polymerase II, such as poly-A tail and cap modification. These plasmids are carrying two different yeast antibiotic resistance genes, G418 and nourseothricin resistance, allowing to maintain the plasmids only for the time of the genome editing, as they are easily lost when cells are moved to non-selective media. This approach is useful to prevent off-targets and toxicity linked to Cas9 endonuclease activity.

We searched for a 20 nucleotides gRNA in the region of interest, after the Sm-like domains and before the C-terminal domains of the *LSM4* yeast gene to recreate the truncated form of *LSM4*, with the bioinformatic tool Benchling © and found a PAM region at 242 nt (87 aa) (Supplemental Figure 3), then we cloned the gRNA in the pCfB2311 plasmid according to Stovicek et al, 2015 (Figure 20, Panel A, right plasmid). The phosphorylated primers used are listed in Table 4 (gRNA highlighted in bold) and the correct substitution of the gRNA was confirmed by sequencing (Supplemental Figure 4). Afterwards, to create the donor DNA cassette we designed a specific pair of primers (Table 4) having at 5'-end 40 bp of homology with the *LSM4* gene in the area surrounding the PAM of interest to promote the genome recombination, while at 3'-end they annealed to the GFP-CYC1 sequence on the pUG35-URA plasmid to use it as a PCR template (Figure 20, Panel B). The resulting construct at genome level after the editing is reported in Figure 20, Panel C. We choose to create the *lsm4Δ1*-GFP cassette in order to easily follow the protein expression using anti-GFP antibody, as the anti-Lsm4 antibodies on the market are polyclonal, resulting not specific for the truncated form, and not validated in yeast.

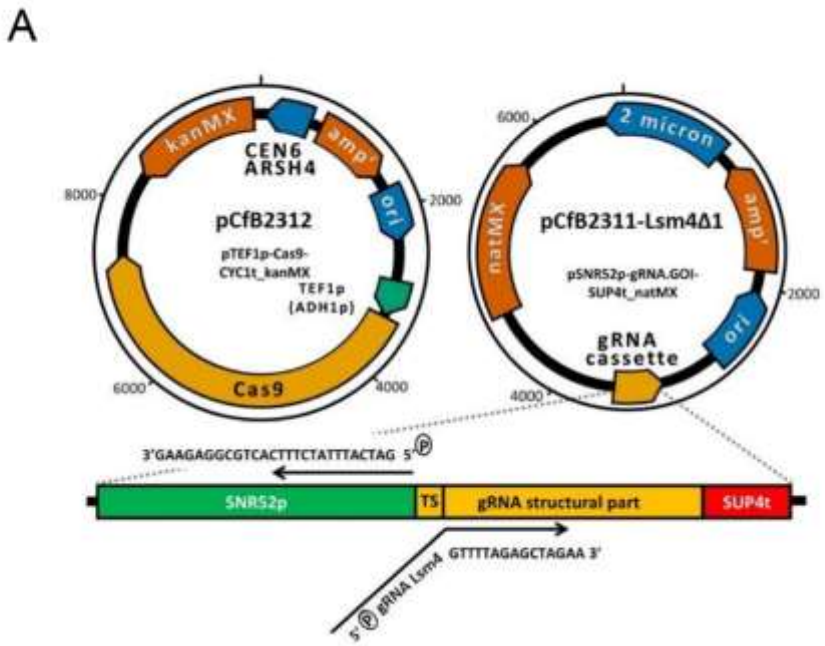

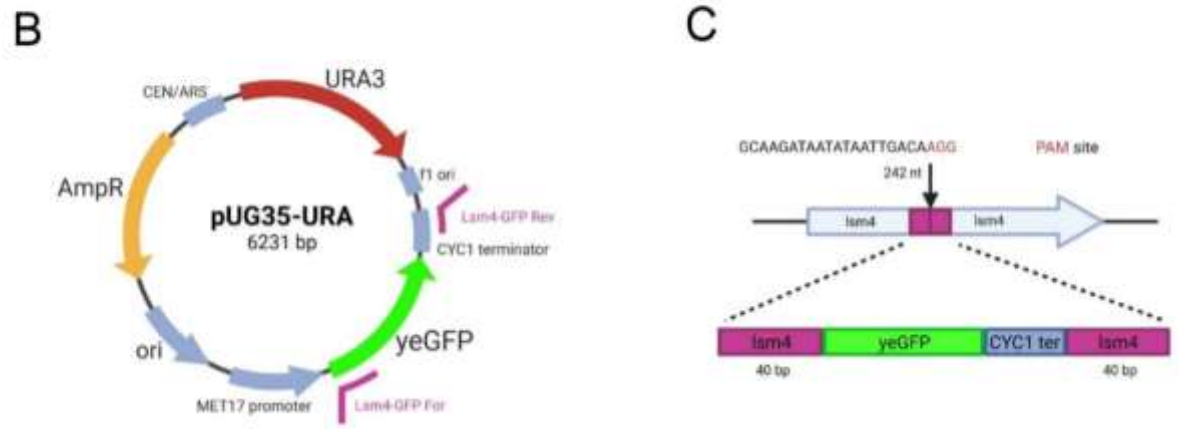

Figure 20. Construction of the *lsm4Δ1*-GFP genome mutant. **(A)** The gRNA of interest (gRNA Lsm4) was cloned in the pCfB2311 plasmid according to (Stovicek, Borodina and Forster, 2015) to give rise to the pCfB2311-*lsm4Δ1* plasmid (right). **(B)** The plasmid pUG35-URA was used as template for the donor PCR, using primers with 40 bp 5'-tails homologous to *LSM4* gene near the Cas9 cut site (PAM site). The resulting donor PCR fragment, and the site of genome recombination, is schematised in Panel **(C)**. Panel (A) adapted from Stovicek, Borodina and Forster, 2015; panels (B) and (C) created in BioRender.com

To expand our knowledge in other genetic contexts, we sequentially transform the BY4741 yeast strain with the pCfB2312 plasmid, pCfB2311-Lsm4Δ1 plasmid and *lsm4Δ1*-GFP donor DNA, and obtained colonies were tested for the correct integration of the cassette (primers listed in Table 4). The cassette, comprising the GFP, CYC1 terminator and Lsm4 tails is 1000 bp long, allowing to easily screen the transformed cells through a PCR. As seen in Figure 21, panel A, the editing efficiency was >70%, with 5 positive colonies over a total of 7 that showed a 1000 bp longer PCR product compared to the wild type BY4741 strain (Lane 8). The PCR products were then purified and sequenced, and results confirmed the perfect recombination of the donor cassette at nucleotide level (Supplemental Figure 5). The obtained *lsm4Δ1*-GFP strain was tested for the effective production of the reporter protein GFP by Western Blot on the protein content of three different *lsm4Δ1*-GFP colonies, and the expression of the fusion protein of around 36.4 kDa was confirmed in all samples (Figure 21, panel B).

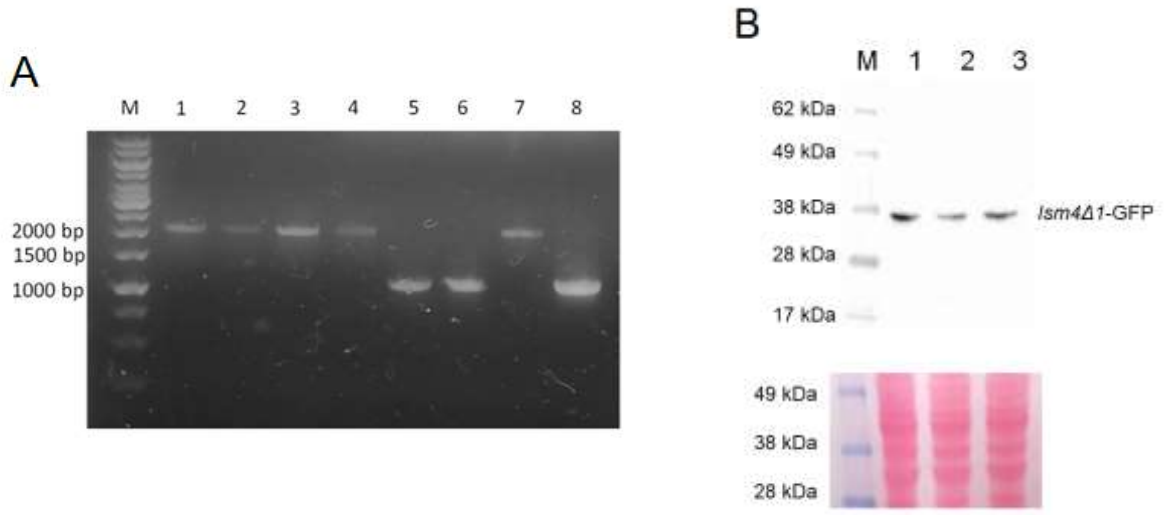

Figure 21. (A) Control PCR on 7 different colonies of BY4741 edited with CRISPR/Cas9 to obtain the *lsm4Δ1*-GFP strain. The PCR fragment in the wild type BY4741 strain (Lane 8) is 1000 bp long, while the edited samples present additional 1000 bp corresponding to the *lsm4Δ1*-GFP cassette, resulting in a 2000 bp band. Five colonies over seven tested result positive to the integration of the cassette, resulting in editing efficiency above 70%. **(B)** Western Blot against GFP of three different colonies of BY4741 *lsm4Δ1*-GFP strain obtained with genome editing. The predicted molecular weight of the fusion protein is 36.4 kDalton and a corresponding band is present in all three samples, confirming the expression of the fusion protein. Ponceau S staining was used as loading control.

5.9 The *lsm4Δ1*-GFP strain shows phenotypes similar to MCY4/*Sclsm4Δ1* mutant strain

The genome-edited strain was analysed at fluorescent microscope to evaluate some of the phenotypical markers of regulated cell death, such as nuclei fragmentation ad accumulation of reactive species of oxygen (ROS) during exponential and stationary phases of growth. As we can see in Figure 22, the mutant strain presents a significant higher percentage of nuclear fragmentation compare to the wild type strains (BY4741 and BY4741/*LSM4*-GFP), both in the exponential and stationary phase, but when compared with the results obtained with the MCY4/*Sclsm4Δ1* strain (Figure 6), the entity of the fragmentation during stationary phase is lower, as the percentage of fragmented nuclei in the *lsm4Δ1*-GFP strain reached 13.4% versus nearly 40% of MCY4/*Sclsm4Δ1.* The differences between the two mutant strains slightly decreased when we analysed the positivity to the DHR-123 staining, which highlights the presence of ROS inside the cells. In fact, the *lsm4Δ1*-GFP showed nearly 13% and 30% of positivity during exponential and stationary phase, respectively, while the MCY4/*Sclsm4Δ1* presented 12% and 60% of ROS positive cells in the same conditions. When compared to its wild type strains, the *lsm4Δ1*-GFP strain showed about 3.5-fold and 13-fold higher percentage of ROS positive cells compared to BY4741

and BY4741/*LSM4*-GFP, respectively, in both growth phases, confirming the similarity in phenotypes with the previously described mutant strain.

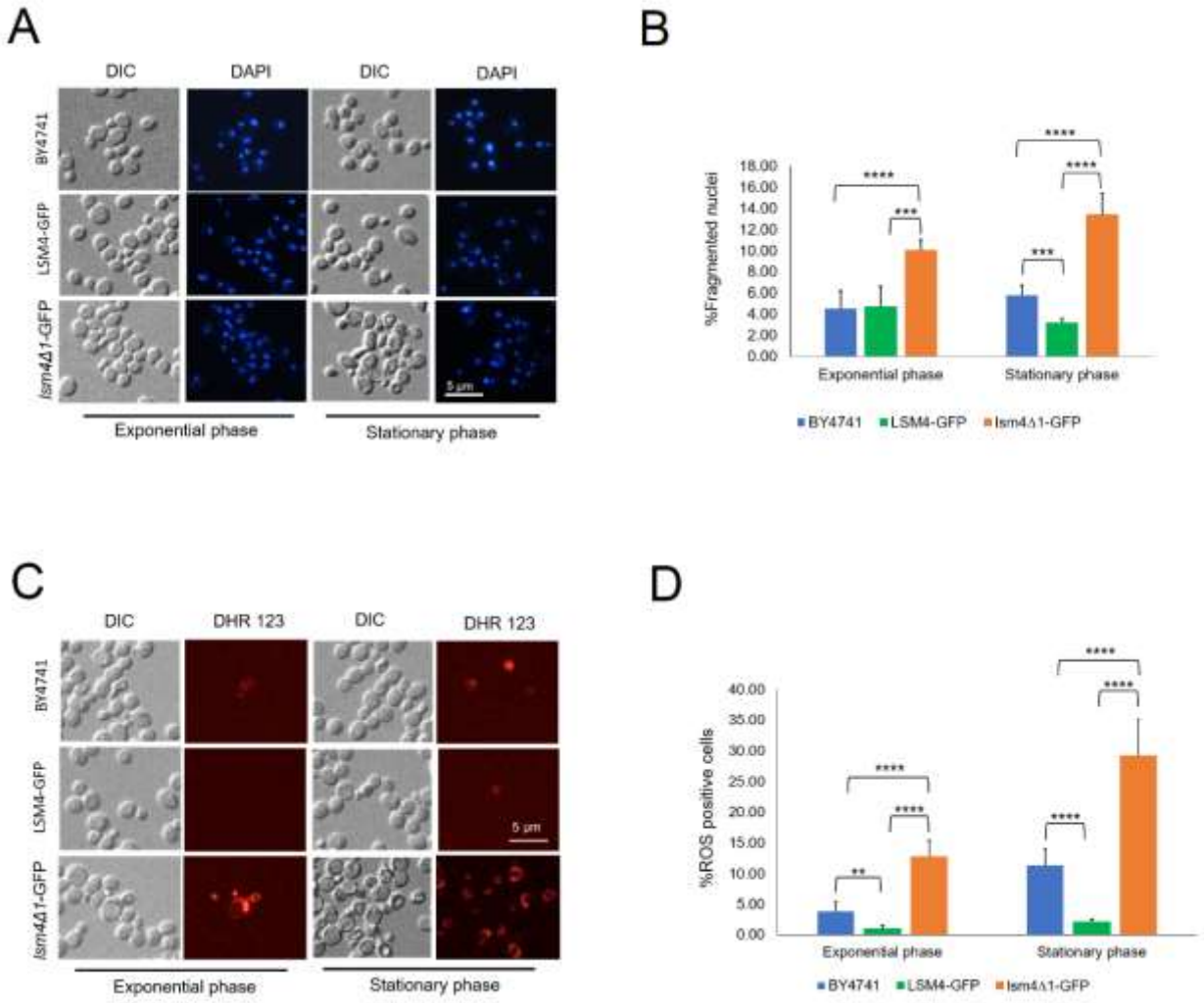

Figure 22. (A) DAPI staining of the BY4741, BY4741/*LSM4*-GFP (wild types) and BY4741/*lsm4Δ1*-GFP mutant cells, in both exponential and stationary phase, quantification of the percentage of fragmented nuclei over total cells from three independent experiments is plotted in **(B)**. **(C)** Dihydrorhodamine 123 (DHR-123) staining of the BY4741, BY4741/*LSM4*-GFP (wild types) and BY4741/*lsm4Δ1*-GFP mutant cells in both exponential and stationary phase, quantification of the percentage of ROS positive cells over total cells from three independent experiments is plotted in **(D)**. Data are represented as mean percentage of 700 cells per set ± standard deviation. **pvalue<0.01 ***p-value<0.001, ****p-value<0.0001

The *lsm4Δ1*-GFP strain was then tested for sensitivity to different compounds in order to evaluate additional similarities with the MCY4/*Sclsm4Δ1* strain. Interestingly, it resulted more resistant to the same concentration of acetic acid (60 mM), as it can grow up to the 10^{-3} dilution (Figure 23), while the MCY4/*Sclsm4Δ1* strain rapidly loses viability after the first dilution (Figure 7), which is

in line with the results obtained with the DHR-123 staining (Figure 22, panel C and D). On the other hand, the sensitivity to caffeine is very high when compared to its wild type BY4741, which per se showed an overall greater survival on caffeine 0.25% compared to the CML39-11A strain. The sensitivity to 6 nM rapamycin was indeed slightly lower compared to the MCY4/*Sclsm4Δ1* strain, but still two-fold higher compared to the BY4741 strain. Given the informations obtained from past experiments on MCY4/*Sclsm4Δ1*, these results suggest that the autophagy process could be impaired also in the *lsm4Δ1*-GFP strain. The BY4741/*LSM4*-GFP was used as additional wild type strain to ensure that the GFP protein does not interfere with the assembly of LSM complexes with consequences on the cells' fitness.

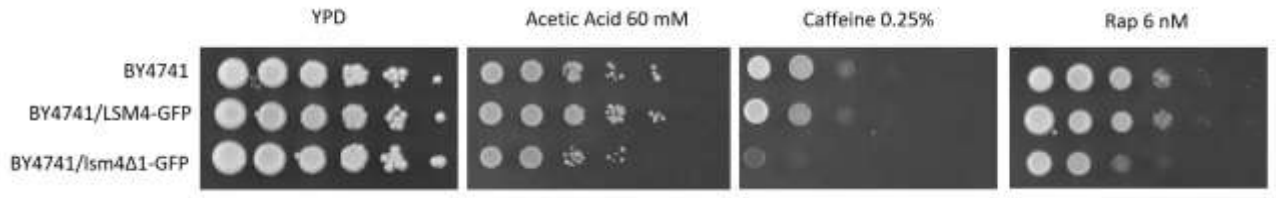

Figure 23. 10-fold dilution of exponential growing cultures in YPD of BY4741 (wild type), BY4741/*LSM4*-GFP and BY4741/*lsm4Δ1*-GFP mutant cells were spotted on complete solid media YPD containing 60 mM acetic acid, 0.25% caffeine and 6 nM rapamycin and plates were incubated at 28°C for 3 days. YPD was used as growth control.

5.10 The *lsm4Δ1*-GFP strain shows higher level of *lsm4Δ1*-GFP protein under nitrogen starvation compared to SD

One of the main advantages of the creation of the *lsm4Δ1*-GFP fusion protein is the possibility to use an easily available antibody against the GFP protein to evaluate the production of the *lsm4Δ1* protein. We therefore analysed the expression of the chimerical protein in SD medium and in SD-N medium, during the exponential phase (4 hours from inoculation in SD and SD-N) and during the post-diauxic phase (22 hours from inoculation). The overall protein content was lower in the nitrogen depleted medium as expected, as we can see from the Ponceau S staining of the membrane, suggesting the slowdown in protein synthesis subsequent to TORC1 inhibition and autophagy activation. Despite this, the expression of the *lsm4Δ1*-GFP protein resulted expressed at the same level compared to the SD cultured cells, suggesting the activation of the *lsm4Δ1*-GFP protein production in nitrogen starvation condition.

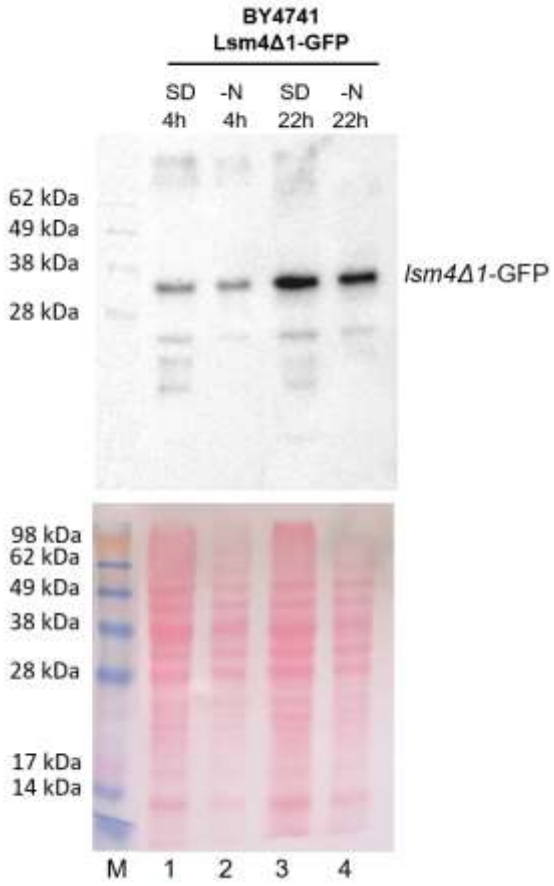

Figure 24. Western blot analysis on cellular extracts of BY4741/*lsm4Δ1*-GFP in nitrogen starvation condition (SD-N), after 4 hours of incubation (lane 2) and 22 hours of incubation (lane 4). SD medium was used as control. Ponceaus S staining was used as loading control.

6. Discussion

Ageing is a complex and dynamic process that can be challenging to study due to the intricate pathways and networks involved, that include both genetic and environmental factors. Therefore, the use of the yeast *Saccharomyces cerevisiae*, that it has always been chosen for its simple maintenance and manipulation together with its incredibly high level of conservation of higher eukaryotic processes and features, has improved and simplified the study of physiological and pathological conditions. The yeast model strain of choice in our laboratory to study cellular ageing has been the *Saccharomyces cerevisiae* strain MCY4, which carries the *LSM4* essential gene under *Gal1-10* promoter control, transformed with a *K. lactis* truncated form of the protein (*Kllsm4Δ1*) on the centromeric pRS313 plasmid to allow the growth on glucose as a carbon source. The Lsm4 protein is part of two essential complexes, which are conserved from yeast to human, that exerts their function in the cytoplasm, the LSM1-7 complex, and in the nucleus, the LSM2-8 complex (Wilusz and Wilusz, 2013). The cytoplasmic LSM complex is involved in the regulation of the decapping process and mRNAs degradation as in thermosensitive mutants of Lsm1-7 proteins, mRNAs are stabilized and it has been demonstrated their association with the decapping complex proteins Dcp1 and Pat1 (Tharun *et al.*, 2000). Moreover, our past studies revealed that the functional part of a single subunit of the cytoplasmic LSM complex is the C-terminal Q/N-rich domain, as the expression of the truncated protein *Kllsm4Δ1* that lacks this particular domain dramatically inhibits the RNA degradation and alters the P-bodies localization (Mazzoni, Mancini, Verdone, *et al.*, 2003; Mazzoni *et al.*, 2005; Mazzoni, D'Addario and Falcone, 2007). As result of the impossibility to properly regulate the degradation of mRNAs, the MCY4/*Kllsm4Δ1* strain shows premature loss of viability and higher content of reactive species of oxygen, together with other typical markers of regulated cell death such as nuclei and DNA fragmentation (Mazzoni, Mancini, Verdone, *et al.*, 2003). The RNAs modification, clearance and degradation are also essential for the maintenance of cellular homeostasis, as a number of stress-responsive cellular pathways are regulated post-transcriptionally to promote a rapid and fine-tuned response (Hernández-Elvira and Sunnerhagen, 2022). Moreover, mammalian genes involved in the regulation of cell cycle are tightly regulated at transcriptional and post-transcriptional level, stressing the importance of mRNAs regulation also in cellular pathways involved in the insurgence of human diseases (Guhaniyogi and Brewer, 2001).

One of these pathways is the autophagy process, which is a highly conserved pro-survival process that mediates the clearance of damaged organelles, proteins and macromolecules through the remodelling of intracellular membranes and delivery of the damaged cargo into digestive organelles, such as lysosomes in mammals and vacuole in plants and yeasts (Klionsky and Emr, 2000; Ryter, Cloonan and Choi, 2013). The regulation of the autophagy pathway is highly intricate, as it has to face different types of cellular stress both external and internal, and a great number of

different stress-sensing factors are able to converge their action into the autophagosomal formation (Lei *et al.*, 2022).

Under nutrient stress, and in particular nitrogen and aminoacids starvation, one of the possible autophagy trigger relies on the proper regulation of the decapping process (Hu *et al.*, 2015), and has been demonstrated the involvement of Lsm proteins in the autophagic process (Costanzo *et al.*, 2010; Mazzoni and Falcone, 2011; Mitchell *et al.*, 2013), corroborated by the evidences reported in (Palermo *et al.*, 2015), in which the overexpression of the autophagy-related protein Nuclear Envelope Morphology protein 1 (*NEM1*) restored most of the aberrant phenotypes found in the *Kllsm4Δ1* expressing strain. This research study is therefore focused on the characterization of the correlation between autophagy and Lsm proteins. Firstly, we constructed the MCY4/*Sclsm4Δ1* strain to have a more physiological scenario and we tested the similarities in phenotypes with the previously described *Kllsm4Δ1* strain. The viability of the MCY4/*Sclsm4Δ1* strain is very short compared to its isogenic wild type CML39-11A, while the expression of the full-length *LSM4* gene (MCY4/*ScLSM4*) restore the lifespan at wild type level (Figure 5), confirming that the loss of viability is not due to the use of the MCY4 strain itself but relies on the truncation of the *LSM4* gene, as already described for the *K. lactis* form (Mazzoni *et al.*, 2005). Furthermore, mutant cells show aberrant morphology, with the loss of the rounded shape typical of yeasts' cells, probably due to problems in the remodelling of internal and external structures, and the nuclei appear enlarged, diffused or fragmented (Figure 6, panel A). The percentage of fragmented nuclei increases as the population of cells progresses in later stages of growth, and even if it is true also for the wild type strain as it is a hallmark of cellular ageing and demise, the mutant cells reach over the 35% of fragmented nuclei in only two days of culture, confirming the rapid accumulation of DNA damage that can concur to the short lifespan of the strain. Another important feature of the MCY4/*Sclsm4Δ1* strain is the early accumulation of reactive species of oxygen (ROS) (Figure 6, panel C). The expression of the truncated form of Lsm4 has no relevant effect on the nuclear splicing process, as the N-terminal Sm-like domains are maintained, while the absence of the C-terminal Q/N-rich domain has a dramatic effect on the cytoplasmic activity of the LSM1-7 complex. The mRNAs unable to be degraded accumulate in the cytoplasm, and they are easily target of oxidation which in turn increases the cellular stress and promotes the entrance in a regulated cell death process. Therefore, the mutant cells are highly sensitive to acetic acid and to even mild oxidative stress, as reported in Figure 7 and 8, while the expression of the full-length Lsm4 protein restores the sensitivity to a wild type level, suggesting the recovery of oxidated mRNAs processing. Moreover, the MCY4/*Sclsm4Δ1* shows a growth defect on glycerol containing medium (Figure 7), defect which is partially recovered in the MCY4/*ScLSM4* strain, suggesting an intrinsic problem of growth on a non-fermentable carbon source of the MCY4 strain that is aggravated by the mutation.

The autophagy process in this context could be crucial for the degradation of bulk RNAs, and it has been reported that reactive species of oxygen could regulate the activity of Atg4 (Pérez-Pérez *et al.*, 2014). Atg4 is a protease that mediates the cleavage of Atg8 protein, allowing the conjugation of

phosphatidylethanolamine (PE) essential for phagophore expansion (Geng and Klionsky, 2008). Moreover, the transcriptional factor Yap1 which mediates the oxidative stress responsive pathway, has been found to positively regulate the transcription of the *ATG15* gene, which is a vacuolar phospholipase that promote the degradation of membrane lipids in the vacuole after the autophagosome-vacuole fusion (Ramya and Rajasekharan, 2016). We therefore wanted to assess if the autophagic process was in some sort non-functioning. As expected, the mutant strain resulted highly sensitive to caffeine (Figure 7), which has been reported to be an outcome of highly perturbed TOR signalling (Kumar *et al.*, 2019) and when we tried to culture the cells in a medium lacking the nitrogen source (SD-N), we reported a shorter lifespan of the mutant strain, while the wild type showed a fairly longer lifespan (Figure 13, panel A), thanks to the proper activation of the autophagy process that mediates the degradation and recycle of damaged structures which in turn promotes the wellness and increases the fitness of the cell population.

The defects in the autophagy process of the MCY4/*Sclsm4Δ1* strain has also been reported through the GFP-Atg8 processing assay. In fact, as seen in Figure 12, the nutrient stress represented by a medium lacking the nitrogen source (SD-N) or the carbon source (S-glu) is not able to trigger the cleavage of the fusion protein GFP-Atg8, suggesting that the autophagic process is defective in one or more of its steps.

As the autophagy pathway involves a great number of proteins, about 31 autophagy-related proteins (Atg) plus all the stress-sensing complexes such as TORC1, membrane biogenesis and remodelling factors such as Nem1/Spo7, and vesicles trafficking regulators, the understanding of the defective step could be challenging and of great interest at the same time. As already mentioned, the overexpression of *NEM1* restores some of the aberrant phenotypes of the *Kllsm4Δ1* expressing strain in nutrient rich conditions, suggesting a problem in membrane biogenesis (Palermo *et al.*, 2015). Therefore we focused our study on the autophagosome formation and its delivery to the vacuole, using the same reporter system GFP-Atg8 and fluorescent microscopy. The cells were cultured with and without the nitrogen source in order to powerfully induce the autophagy pathway and force the delivery of the fluorescent protein inside the vacuole. At first the fluorescence was homogeneously distributed in the cytoplasm in both the wild type and the MCY4/*Sclsm4Δ1* strain, then after four hours in SD-N medium the percentage of cells presenting GFP dots outside the vacuole increased to a greater extent in the mutant (Figure 14, panel A). As the growth of the cultures proceeded in both SD and SD-N media, the fluorescence was mainly found in the vacuolar compartment in the wild type strain, while in the mutant the percentage of dots-positive cells increased, strongly excluding the cellular vacuoles (Figure 14, panels C and E). The green fluorescence represented the localization of the Atg8 protein, therefore we can infer that in the wild type the presence of scarce nutrient or ageing of the culture are able to properly trigger the autophagy pathway and the formation of the autophagosomes, and their consequent delivery to the vacuole works as expected. On the other hand, the same conditions in the MCY4/*Sclsm4Δ1* strain led to the accumulation of cytoplasmic structures, suggesting that the autophagosome formation is maintained and the limiting step relies on the transport of the cargo to the final

compartment. This is also true in a deletion mutant for the *LSM1* gene, of which protein product is component only of the cytoplasmic LSM complex. The *lsm1Δ* strain, in fact, showed similar dots accumulation in both media: the percentage of dots-positive cells were slightly lower compared to the *Sclsm4Δ1* expressing strain, but the number of dots per single cells resulted higher (Figure 15). This result could be explained by the intrinsic differences between genetic backgrounds, as their wild type strains, CML39-11A for MCY4/*Sclsm4Δ1* and BMA38 for *lsm1Δ*, showed differences in the percentage and number of dots as well. Despite these minor differences, we can assert that in yeast strains defective in mRNAs degradation due to cytoplasmic LSM complex mutations, the translocation of the autophagosome or its fusion with the vacuole is impaired, with dramatic consequences for the fitness of the cell when it is exposed to nitrogen starvation.

On the other hand, when cells were cultured under calorie restriction, we saw an incredible increase in life span of both mutant and wild type strains (Figure 13, panels B and C). The elongation of life span under dietary restriction is now well-established (Fontana, Partridge and Longo, 2010), but many are the mechanisms that can concur to this process. The energy stress derived from a minor intake of glucose, in fact, is able to activate the action of ATP-sensing kinases, such as AMPK in mammals and SNF1 in yeast, that can trigger the autophagy pathway via direct phosphorylation and inhibition of MTOR (Gwinn *et al.*, 2008) or via the phosphorylation and activation of TOR upstream negative regulator TSC2 (Inoki, Zhu and Guan, 2003). At the same time, the reduced glycolysis affects the NAD+/NADH ratio, with a great accumulation of NAD+ that promotes the activation of NAD+ dependent histone deacetylase Sir2 (Landry *et al.*, 2000). Other than its well-known role in transcriptional silencing of the silent mating loci, telomeres, and rDNA recombination (Guarente, 1999), Sir2 is involved in the elongation of the life span under calorie restriction through the activation of autophagy (Morselli *et al.*, 2010; Sampaio-Marques *et al.*, 2012) and it is also under the regulation of AMPK/SNF1. Taken these data together, it is possible that this energy-mediated trigger of autophagy is still working in our mutant strain, and further analysis need to be done to confirm this hypothesis.

As the MCY4/*Sclsm4Δ1* strain accumulates mRNAs not able to be degraded, we searched for other processes that could mediate the clearance of bulk RNAs through extracellular secretion. In animals, one of the possible and regulated way to transfer nucleic acids in the extracellular compartment is the production of extracellular vesicles (EVs), and they are mostly involved in intercellular communication (O'Grady *et al.*, 2022). In fact, they can be packed with coding or regulatory RNAs that can be taken up by surrounding cells thereby facilitating the exchange of information, and recent studies demonstrate their critical role also in physiological and pathological processes, such as neural development, secretion and propagation of prions and amyloid fibrils and tumour progression (Rajendran *et al.*, 2014). Although the first evidences of the presence of EVs in yeast are from the 1970s (Gibson and Peberdy, 1972), their biogenesis process is still unclear, and proteins homologous to tetraspanins, well known surface markers of mammals

EVs, have not yet been found. On the other hand, the crucial role of EVs in yeast communication and pathogenesis is now well established, in fact recent studies demonstrate their participation in the delivery of virulence factors, prion-like proteins and cell wall remodelling enzymes (Rodrigues *et al.*, 2011; Kabani and Melki, 2016; Zhao *et al.*, 2019), but our interest was mainly captured by a work that demonstrated the secretion via EVs of small and fragmented RNAs (Peres da Silva *et al.*, 2015). Inspired by these works, we preliminarily analysed the nucleic acid content of the supernatant of the *LSM4* mutant cultures and saw the accumulation of small or fragmented RNAs after four days of extreme calorie restriction, while in the wild type control the enrichment was not detectable (Figure 17). In addition, we analysed the RNA content of the supernatants of cells cultured on solid SD medium, as a recent study demonstrated the production of extracellular vesicles in this condition and proposed a novel protocol for their isolation from agar plates (Reis *et al.*, 2019). Again, the wild type strain did not show any RNA secretion, while the MCY4/*Sclsm4Δ1* strain showed a great production of extracellular RNAs (Figure 18). Interestingly, we observed a different enrichment in RNA content based on the filtration size used, suggesting the association of the nucleic acid with vesicles of different size. Moreover, the mutant strain showed large extracellular structures during chronological ageing compared to the wild type, which could represent a specific kind of extracellular vesicles, such as apoptotic bodies (Figure 19), but in depth analysis, such as Nanoparticle Tracking Analysis (NTA) need to be performed to confirm this hypothesis.

Despite this promising result, whether these RNAs are secreted through regulated extracellular vesicles is not clear yet, but their predominant secretion in the mutants' supernatants in extreme calorie restriction could represent a new survival process in a system where the degradation of RNAs by the decapping machinery and the autophagic pathway are compromised.

In parallel to these experiments, we wanted to construct a yeast strain carrying the *LSM4* truncation at genome level, in order to eliminate the dependence from the carbon source or auxotrophic selection and prevent any possibility of reactivation of the full-length form transcription. We edited the BY4741 DNA through the CRISPR/Cas9 method optimized by (Stovicek, Borodina and Forster, 2015) using a guide-RNA (gRNA) complementary to the zone of truncation (after the zone encoding the Sm-like domains but upstream of the Q/N-rich domain) in order to obtain a mutant yeast strain as similar as possible to the MCY4/*Sclsm4Δ1* strain. We designed the donor cassette used for the recombination with *LSM4* tails flanking the *GFP* and its terminator from a commonly used expression vector (pUG35-URA) to permit different protein analysis (Western Blot, ELISA, IP etc.), as it is not available a specific antibody for the truncated form of Lsm4. The resulting strain has successfully shown similar phenotypes compared to the MCY4/*Sclsm4Δ1* strain regarding ROS accumulation and nuclei fragmentation, while in terms of viability it is still under analysis. Interestingly, it shows a very high sensitivity to caffeine and rapamycin, suggesting that it could present similar autophagic defects that could confirm again the involvement of the LSM proteins in this process. Unfortunately, even if the *lsm4Δ1*-GFP and the GFP-Atg8 fusion proteins theoretically present a quite different molecular weight (36.5 kDa and 41

kDa respectively), we were not able to distinguish them through Western Blot analysis because of the great accumulation of the GFP-Atg8 protein already seen also in the MCY4/*Sclsm4Δ1* mutant strain (Supplemental Figure 6), making difficult to perform the same autophagic induction assay. Therefore, different analysis need to be done to confirm the autophagic defects in this strain. As an interesting and promising final result, we preliminary analysed the expression of the *lsm4Δ1*-GFP protein during nitrogen starvation through Western Blot analysis and we saw an enrichment in protein synthesis in this condition compared to the SD medium (Figure 24). This important result could represent the missing link between the defects in autophagy and the truncated Lsm4 protein, as it seems to be upregulated in a strong autophagy inducing condition, and it opens exciting new horizons in the study of the correlation between decapping mutants, ageing and autophagy.

7. Materials and methods

Yeast strains, growth conditions and plasmids construction

Saccharomyces cerevisiae strains used in this work are described in Table 1. Cells were grown at 28°C in YPD (1% yeast extract (BD, #212750), 2% bacto-peptone (BD, #211677), 2% glucose), SD (0.67% yeast nitrogen base without aminoacids (BD, #291940), 2% glucose) supplemented with auxotrophic requirements. YPY medium (1% yeast extract (BD, #212750), 2% bacto-peptone (BD, #211677), 2% glycerol) was used to evaluate growth on glycerol as a carbon source. For autophagic induction by nitrogen starvation cells were grown in SD-N (0.17% yeast nitrogen base without aminoacids and ammonium sulphate (BD, #233520), 2% glucose). For autophagy induction on calorie restriction experiments cells were grown in S-glu (0.67% yeast nitrogen base without aminoacids (BD, #291940)) supplemented with auxotrophic requirements. For survival tests during chronological life span (CLS) under calorie restriction condition, cells were grown in SD 0.1% (0.67% yeast nitrogen base without aminoacids (BD, #291940), glucose 0.1%) supplemented with auxotrophic requirements and distilled sterilized water. Solid media were obtained by the addition of 2% Bactoagar (BD, #214010).

Escherichia coli strain DH5α used for the propagation of plasmid DNA is listed in Table 2. Bacterial cells were grown at 37°C in LB medium (0.5% yeast extract (BD, #212750), 1% tryptone (BD #211705), 0.5% NaCl) supplemented with 100 μg/ml ampicillin.

Plasmid pRS313/*Sclsm4Δ1* was obtained by amplifying 868 bp of the *ScLSM4* gene, comprising the promoter region and the gene portion encoding the first 84 aminoacids, and then cloning the PCR fragment with BamH1/SacI extremities in the specific site of the vector (primers listed in Table 3).

Plasmid pRS313/*ScLSM4* was obtained by amplifying 1308 bp of the *ScLSM4* gene, comprising the promoter region and the complete coding region, and then cloning the PCR fragment with BamH1/SacI extremities in the specific site of the vector (primers listed in Table 3).

Plasmid pUG36/*ATG8* was a courtesy of T. Eisenberg and colleagues (Eisenberg *et al.*, 2009).

Plasmid pUG35-URA was a courtesy of J. H. Hegemann, Heinrich-Heine-Universitat, Dusseldorf, Germany.

Plasmids pCfB2312 and pCfB2311 were purchased through AddGene from Irina Borodina and colleagues (Stovicek, Borodina and Forster, 2015). Transformation of the selected strain was performed by PEG/LiAc method according to Gietz and Woods (Gietz and Woods, 2006).

Transformation with pRS313/*Sclsm4Δ1*, pRS313/*ScLSM4* and pUG36/*ATG8* was performed by ONE-STEP method with ONE-STEP buffer (PEG 3350 40%, LiAc 0.2 M, DTT 0.1 M and ssDNA carrier 0.1 μg/μl (Sigma-Aldrich, D1626)) as transformation mix (Chen, Yang and Kuo, 1992).

To determine the growth rates in rich medium, MCY4/*Sclsm4Δ1,* MCY4/*ScLSM4* and CML39-11A strains were grown exponentially on YPD and OD_{600} values were taken every two hour. The growth rate (μ) was calculated as $(\ln N_t - \ln N_0) / (t - t_0)$ within the intervals 4h-6h and 6h-8h and then mediated. Results are reported in Figure 4.

To observe the apoptotic bodies, cells were grown on liquid YPD and then $3x10^3$ cells plated on YPD agar coated slide, then incubated at 28°C for five days and analysed at the microscope (Axioskop 2, Carl Zeiss, Germany).

Table 1. *S. cerevisiae* strains used in this work.

Strain	**Genotype**	**Source**
MCY4	*MATα, ade1-101, his3-Δ1, trp1-289, ura3, LEU-GAL1-SDB23*	(Cooper, Johnston and Beggs, 1995)
MCY4/Sc*lsm4Δ1*	*MATα, ade1-101, his3-Δ1, trp1-289, ura3, LEU-GAL1-SDB23* pRS313/Sc*lsm4Δ1*	This work
CML39-11A	*MAT*a, *ade1-101, his3-Δ1, leu2, ura3, trp1-289*	(Mazzoni *et al.*, 2005)
MCY4/*ScLSM4*	*MATα, ade1-101, his3-Δ1, trp1-289, ura3, LEU-GAL1-SDB23* pRS313/*ScLSM4*	This work
MCY4/Sc*lsm4Δ1* pUG36/*ATG8*	*MAT α, ade1-101, his3-Δ1, trp1-289, ura3, LEU-GAL1-SDB23* pRS313/Sc*lsm4Δ1*, pUG36/*ATG8*	This work
CML39-11A pUG36/*ATG8*	*MAT a, ade1-101, his3-Δ1, leu2, ura3, trp1-289* pUG36/*ATG8*	This work
MCY4/Sc*LSM4* pUG36/*ATG8*	*MAT α, ade1-101, his3-Δ1, trp1-289, ura3, LEU-GAL1-SDB23* pRS313/*ScLSM4*, pUG36/*ATG8*	This work
BMA38	*MAT α, ura3-1, leu2-3, -112, ade2-1, can1-100, his3-11, -15, trp1Δ1*	(Tsukada and Ohsumi, 1993)
BMA38 *lsm1Δ*	*MAT α, ura3-1, leu2-3, -112, ade2-1, can1-100, his3-11, -15, trp1Δ1, lsm1Δ::TRP1*	(Tsukada and Ohsumi, 1993)
BY4741	*Mat a, his3-Δ1, leu2-Δ0, met15-Δ0, ura3-Δ0*	(Brachmann *et al.*, 1998)
BY4741 pUG36/*ATG8*	*Mat a, his3-Δ1, leu2-Δ0, met15-Δ0, ura3-Δ0* pUG36/*ATG8*	This work

BY4741 LSM4-GFP	*Mat a, his3-Δ1, leu2-Δ0, met15-Δ0, ura3-Δ0*	Euroscarf
BY4741 *lsm4Δ1*-GFP	*Mat a, his3-Δ1, leu2-Δ0, met15-Δ0, ura3-Δ0, lsm4Δ1::GFP*	This work
BY4741 *lsm4Δ1*-GFP pUG36/*ATG8*	*Mat a, his3-Δ1, leu2-Δ0, met15-Δ0, ura3-Δ0, lsm4Δ1::GFP* pUG36/*ATG8*	This work

Table 2. *E. coli* strain used in this work.

Strain	**Genotype**	**Source**
DH5α	*dlacZ Δ M15 Δ(lacZYA-argF) U169 recA1 endA1 hsdR17(rK-mK+) supE44 thi-1 gyrA96 relA1*	(Taylor, Walker and McInnes, 1993)

Table 3. Amplification and cloning of the N-terminus truncated *Sclsm4Δ1* gene and the full length *ScLSM4* gene.

Primer Name	**Oligonucleotide Sequence**
BamH1-ScLSM4/*Sclsm4Δ1* Fw	5'-AAAAAAGGATCCGTACGCAGTCACAATGCGG-3'
SacI-ScLSM4 Rv	5'-GGGGGGAGCTCACCTGTAAACTAAAGGAAAGCTCG-3'
SacI-Sclsm4Δ1 Rv	5'-GGGGGGAGCTCTTATCTTGCAATTTGATAAACTTGATAAAAGTCC-3'

Viability assays

Stationary cultures of strain MCY4/*Sclsm4Δ1* and CML39-11A were tested for microcolony forming ability during chronological lifespan in SD and SD-N media. Starting from an overnight preculture in 3 ml of SD with auxotrophic requirements, cells were counted and diluted to a final concentration of $5x10^5$ cells/ml in 20 ml of medium (SD or SD-N) and the flasks incubated at 28°C.

Starting from day 1, $3x10^4$ cells were daily plated on a YPD coated slide and analysed with optic microscope after 1-2 days of incubation at 28°C. Cell viability was calculated as the percentage of microcolony forming cells (Palermo, Falcone and Mazzoni, 2007).

Fluorescence microscopy

Nuclear morphology was detected with DAPI staining (1 μg/ml) (Sigma-Aldrich, D8417) of 1 ml of exponentially growing cells (0.2-0.4 OD_{600}) fixed with 70% (v/v) ethanol. Oxygen reactive species (ROS) were detected by incubating 1 ml of cells with 5 μg/ml of DHR 123 (Sigma-Aldrich, D1054) for 4h at 28°C and then analysed at fluorescent microscopy (Axioskop 2, Carl Zeiss, Germany).

The visualisation of autophagosome formation and translocation was performed using the reporter plasmid pUG36/*ATG8* and analysed at the same fluorescent microscopy. The strains of interest were grown in 20 ml SD medium supplemented with auxotrophic requirements and methionine (10 μg/ml), then harvested at their exponential phase (0.2-0.4 OD_{600}), washed with H_2O and splitted in 10 ml of SD medium supplemented with auxotrophic requirements and methionine (10 μg/ml) and 10 ml of SD-N medium without aminoacids. Flasks were incubated at 28°C and then harvested at their logarithmic growth phase (Exp, 0.4 OD_{600}) post-diauxic phase (after 16h, 0.9-1 OD_{600}) and at stationary phase (after 3 days, 1.5 OD_{600}). The percentage of GFP-Atg8 dots positive cells was calculated among the total number of fluorescence-positive cells. The cells were counted manually with ImageJ software (Version 1.8.0_172) (Schneider, Rasband and Eliceiri, 2012).

Glycerol growth, caffeine, acetic acid and rapamycin sensitivity test

Serial dilutions of strains CML39-11A and MCY4/*Sclsm4Δ1* were spotted on YPD, YPY, YPD+0.25% and 0.15% caffeine, YPD+60 mM acetic acid and YPD+6 nM rapamycin and their viability was detected after 2-3 days of incubation at 28°C. Serial dilutions of strains BMA38 and *lsm1Δ* were spotted on YPD, YPD+0.15% caffeine, YPD+60 mM acetic acid and YPD+6 nM rapamycin and their viability was detected after 2-3 days of incubation at 28°C.

H_2O_2 sensitivity test

Starting from an exponential preculture in 20 ml of SD medium with auxotrophic requirements (0.2-0.3 OD_{600}), 1 ml of culture was incubated for 4h at 28°C with 0 mM (control), 0.1 mM, 0.2 mM, 0.5 mM, 0.8 mM, 1.2 mM, 3 mM of H_2O_2 (Sigma-Aldrich, #216763) and then $3x10^4$ cells were plated on a YPD coated slide and analysed with optic microscope after 24 hours of incubation at 28°C. Cell viability was calculated as the percentage of microcolony forming cells.

Rapamycin treatment

Strains MCY4/*Sclsm4Δ1* and CML39-11A were tested for the microcolony forming ability after treatment with 6 nM of rapamycin (Sigma-Aldrich, R8781). Starting from an exponential preculture in 40 ml of SD medium with auxotrophic requirements (0.2-0.3 OD_{600}) cells were splitted in 20 ml SD medium with auxotrophic requirements (controls) or SD with auxotrophic requirements supplemented with 6 nM of rapamycin (test samples). After 1, 2, 3 and 4 hours of treatment, $3x10^4$ cells were plated on a YPD coated slide and analysed with optic microscope after 1-2 days of incubation at 28°C. Cell viability was calculated as the percentage of microcolony forming cells.

Protein extraction and Western Blot analysis

Decapping mutant and the wild type strain were grown on 20 ml SD medium supplemented with auxotrophic requirements and methionine (10 μg/ml), then harvested at their exponential phase (0.2-0.4 OD_{600}), washed with H_2O and splitted in 10 ml of SD medium supplemented with auxotrophic requirements and methionine (10 μg/ml), 10 ml of SD-N medium without aminoacids and S-glu medium with auxotrophic requirements and methionine (10 μg/ml). Flasks were incubated at 28°C and then SD cultured cells were harvested at their logarithmic growth phase (Exp, 0.4 OD_{600}) and post-diauxic phase (after 16h, 0.9-1 OD_{600}), while SD-N and S-glu cultured cells were harvested after 16h. The amount of cells corresponding to 2 OD_{600} were washed with H_2O, resuspended in 200 μl of NaOH 2 M/β-mercaptoethanol 5% and then chilled on ice for 10'. Protein precipitation was performed with TCA at a final concentration of 8.3%, centrifugation at 13000 rpm for 15' and pellet suspended in 100 μl of loading buffer (50 mM Tris-HCl pH 6.8; 100 mM β-mercaptoethanol; 2% SDS, 0.1% bromophenol blue; 10% glycerol). Samples were then boiled at 95°C for 5' and loaded into 12% acrylamide SDS-PAGE gel. A protein marker was loaded in the first lane (Thermo-Fisher, LC5925). Separated proteins were transferred onto nitrocellulose membrane through electroblotting. Ponceau red staining was used as a loading control (0.1% Ponceau S (Sigma-Aldrich, P-3504), 5% acetic acid). Autophagic cargo processing was studied via immunoblotting analysis using anti-GFP antibody (α-mouse-GFP, Santa Cruz Biotechnology, sc-9996) to detect GFP-Atg8, as described in (Daniel J. Klionsky *et al.*, 2021). The secondary antibody HRP-associated was sc-2060 Santa Cruz Biotechnology anti-mouse (goat). Percentage of autophagy activation was determined as the ratio between free GFP and the total GFP (free GFP/free GFP+fusion protein GFP-Atg8), calculated with Image Lab™ Volume Tool Software after the image capture at ChemiDocTM XRS+ System (Bio-Rad).

BY4741 *lsm4Δ1*-GFP colonies were tested for *lsm4Δ1*-GFP protein production through Western Blot analysis. Exponentially growing cells (0.2-0.4 OD_{600}) in YPD medium were harvested and washed with H_2O. Then protein extraction, SDS-PAGE and immunoblotting followed the same protocol as already described using the anti-GFP antibody (α-mouse-GFP, Santa Cruz Biotechnology, sc-9996)

and the secondary antibody HRP-associated anti-mouse (goat) (sc-2060, Santa Cruz Biotechnology).

Construction of lsm4Δ1-GFP genome mutant using the CRISPR/Cas9 editing system

The gRNA of interest was found using the bioinformatic tool Benchling © and then cloned the Lsm4 gRNA of interest in the pCfB2311 plasmid using 5′-phosphorylated primers listed in Table 4 (the gRNA sequence is reported in bold) and the proofreading Velocity DNA Polymerase (Meridian, BIO-21098), swapping the ade2 gRNA already present according to Stovicek et al. 2015. The obtained plasmid pCfB2311-Lsm4Δ1 was transformed into *E. coli* DH5α cells, made competent with $CaCl_2$ method, and positive cells were selected on LB plate supplemented with 100 mg/L ampicillin. Plasmid DNA was extracted with ISOLATE II Plasmid Mini Kit (Bioline, BIO-52056).

Yeast cells were then transformed with pCfB2312 plasmid, containing the Cas9 gene, according to Gietz and Woods, 2006, plated on YPD supplemented with 200 mg/L G418 sulfate and incubated at 28°C for three to four days. Resulting colonies were then double transformed with pCfB2311-Lsm4Δ1 plasmid and donor DNA obtained by PCR on pUG35-URA plasmid (primers listed on Table 4), and plated on YPD supplemented with both 200 mg/L G418 sulfate and 100 mg/L nourseothricin. After 4-6 days at 28°C, resulting colonies were plated on YPD without antibiotics, to allow the loss of plasmids. Screening of colonies was performed through PCR (primers listed on Table 4) and sequencing of PCR products, purified with the Gel/PCR DNA Fragments Extraction Kit (Geneaid, DF100), was committed to Bio-Fab research s.r.l.

Table 4. Primers used in the construction of lsm4Δ1-GFP genome mutant.

Primer Name	**Oligonucleotide Sequence**	**Function**
gRNAlsm4For-P	5′-P-**GCAAGATAATATAATTGACA**GTTTTAGAGCTAGAAATAGCAAGTAAAATAAGGC-3′	Cloning of LSM4 gRNA in pCfB2311 plasmid - Forward
SNR52Rev-P	5′-P-GATCATTTATCTTTCACTGCGGCGAAG-3′	Cloning of LSM4 gRNA in pCfB2311 plasmid - Reverse
Lsm4-GFP For	5′-GGGACTTTTATCATCAAGTTTATCAAATTGCAAGATAATATAATCGATACCGTCGACCTCGAC-3′	Production of donor Lsm4-GFP cassette - Forward

Lsm4-GFP Rev	5′-GGGCCGTTACTATTAGAGTTATTGTTGGAGTTAATTTGCTGACGTTGTAAAACGACGGCC-3′	Production of donor Lsm4-GFP cassette - Reverse
ScLSM4 for	5'-AAAAAAGGATCCGTACGCAGTCACAATGCGG-3'	Screening of transformed yeast colonies - Forward
ScLSM4 rev	5'-TTGGACGGACCCACCTAAAC-3'	Screening of transformed yeast colonies - Reverse

DNA extraction and PCR analysis

The production of the Lsm4-GFP donor and the evaluation of its correct integration at genome level was performed through PCR. Colonies to be tested were harvested from YPD plates and resuspended in 100 µl lysis solution (0.2 M LiAc, 1% SDS) and then incubated at 70°C for 15′. Then TE buffer was added and 300 µl of EtOH 96° was used to precipitate the nucleic acid, and the samples incubated at -20°C for 30′. After a centrifuge at 10000 rpm for 5′, 3 µl of supernatant was used as template for the PCR reaction, using the Accuzyme ™ DNA polymerase (Meridian, BIO-21052) with primers listed in Table 4. Resulting products were separated through electrophoresis on agarose gel, 1% in TAE buffer 1x (40 mM Tris, 20 mM Acetate and 1 mM EDTA).

Total RNA extraction, cDNA syntesis and Real-Time qPCR for mRNA expression of ScLSM4

Strains MCY4/*Sclsm4Δ1,* MCY4/*ScLSM4* and CML39-11A were grown on 20 ml of YPD and harvested at their exponential phase (0.2-0.4 OD_{600}). The amount of cells corresponding to 4 OD_{600} were washed with H_2O, resuspended in 200 µl of lysis buffer (0.5 M NaCl, 0.2 M Tris-HCl pH 7.5, 10 mM EDTA, 1% SDS) and 200 µl of phenol-chlorophorm-isoamyl alcohol (PCI) 25:24:1 (Sigma, 77617) and grounded by vortexing with micro glass beads. After the addition of 300 µl of lysis buffer and 300 µl of PCI, cells were centrifugated at 10000 rpm for 5′ at 4°C, then the supernatant precipitated with 3 volumes of EtOH at -20°C for 30′. The precipitated nucleic acid were resuspended in 15 µl of RNase-free H_2O. The integrity of RNA was tested via electrophoresis on agarose gel, 1% in TAE buffer 1x (40 mM Tris, 20 mM Acetate and 1 mM EDTA) stained with Ethidium Bromide. RNA was treated with DNaseI using the DNA-*free* ™ kit (Invitrogen, AM1906) and retrotrascribed in cDNA using the SensiFAST cDNA Synthesis Kit (Meridian, BIO-65053), according to their datasheets respectively. To evaluate the expression levels of *LSM4*, obtained cDNAs were used as template for a Real-Time qPCR assay, using the primers listed in Table 5, using the SensiFAST SYBR Hi-ROX kit (Meridian, BIO-92020). *TDH3* gene (glyceraldehyde-3-

phosphate dehydrogenase) was used as the calibrator. Datas were obtained at StepOne Plus (Applied Biosystem) and further analyzed with the ΔΔCt method. Results are reported in Figure 4.

Table 5. Primers used in Real-Time qPCR experiment for *ScLSM4* expression.

Primer Name	**Oligonucleotide Sequence**
ScLSM4 N-term Fw	5'-ATTGACCAACGTAGATAACTGGA -3'
ScLSM4 N-term Rv	5'-TACGGCTTTACTGCTCTCAG -3'
TDH3 Fw	5'-CGGTAGATACGCTGGTGAAGTTTC -3'
TDH3 Rv	5'-TGGAAGATGGAGCAGTGATAACAAC-3'

Extracellular RNA extraction

Strains MCY4/*Sclsm4Δ1* and CML39-11A were grown on 20 ml of YPD and harvested at their stationary phase (4.00-6.00 OD_{600}). The amount of cells corresponding to 40 OD_{600} were then washed with H_2O and resuspended in 3 ml of medium of interest (SD supplemented with auxotrophic requirements and H_2O) and incubated at 28°C for four days. Then 2 ml of the culture were centrifuged at max speed (13300 rpm) for 30' at 4°C, and the supernatant filtered at 0.22 μm. To facilitate the RNA extraction from the putative extracellular vesicles, it was used a lysis buffer (Tris Hcl pH 7.4 50 mM; EDTA 5 mM; Triton X-100 1%) and then the nucleic acid precipitation was performed with NaAc 0.3 M, 1 μl glycogen (10 mg/ml) (Thermo Scientific, #R0561) and three volumes of EtOH 96° at -20°C for 20 minutes, then the samples were centrifuged at 13200 rpm for 20 minutes, the pellet washed with EtOH 70% and then resuspended in 15 μl H_2O. For visualization, samples were incubated at 70°C for 10 minutes with 2X RNA loading buffer (Thermo Scientific, #R0641) and loaded on 3% agarose gel stained with Ethidium Bromide.

For extraction of RNAs from cells cultured on solid media, 10^7 cells were plated on SD plates supplemented with auxotrophic requirements and incubated at 28°C for three days. Cells from one plate were then harvested with a sterile scraper and resuspended in 2 ml of PBS, then was followed the protocol described above. Before the RNA precipitation, supernatants were filtered with different filters as described in the text.

Statistical analysis

The presented data show the mean of three independent biological experiments and error bars represent the standard deviation, for the exception of the experiments presented in Figure 4 and in Figure 16, were the mean and standard deviation of two biological replicates are shown. For DAPI and DHR 123 analysis were counted >700 cells per set, for GFP-Atg8 dots analysis were counted >300 cells per set.

To evaluate the statistical significance, it was performed a two-tailed, two sample unequal variance test and the number of stars (*) indicate the p-value range: *p-value <0.05, **p-value <0.01, ***p-value <0.001, ****p-value <0.0001, no star: no statistically significant.

8. References

Arribas-Layton, M. *et al.* (2016) 'The C-Terminal RGG Domain of Human Lsm4 Promotes Processing Body Formation Stimulated by Arginine Dimethylation', *Molecular and Cellular Biology*, 36(17), pp. 2226–2235. Available at: https://doi.org/10.1128/MCB.01102-15.

Brachmann, C.B. *et al.* (1998) 'Designer deletion strains derived from Saccharomyces cerevisiae S288C: a useful set of strains and plasmids for PCR-mediated gene disruption and other applications', *Yeast (Chichester, England)*, 14(2), pp. 115–132. Available at: https://doi.org/10.1002/(SICI)1097-0061(19980130)14:2<115::AID-YEA204>3.0.CO;2-2.

Catalá, R. *et al.* (2019) 'Emerging Roles of LSM Complexes in Posttranscriptional Regulation of Plant Response to Abiotic Stress', *Frontiers in Plant Science*, 10. Available at: https://doi.org/10.3389/fpls.2019.00167.

Cebollero, E. and Reggiori, F. (2009) 'Regulation of autophagy in yeast Saccharomyces cerevisiae', *Biochimica et Biophysica Acta (BBA) - Molecular Cell Research*, 1793(9), pp. 1413–1421. Available at: https://doi.org/10.1016/j.bbamcr.2009.01.008.

Chen, D.-C., Yang, B.-C. and Kuo, T.-T. (1992) 'One-step transformation of yeast in stationary phase', *Current Genetics*, 21(1), pp. 83–84. Available at: https://doi.org/10.1007/BF00318659.

Chen, Z. *et al.* (2021) 'Prognostic value and potential molecular mechanism of the like-Sm gene family in early-stage pancreatic ductal adenocarcinoma', *Translational Cancer Research*, 10(4), pp. 1744–1760. Available at: https://doi.org/10.21037/tcr-20-3056.

Chowdhury, A., Kalurupalle, S. and Tharun, S. (2014) 'Pat1 contributes to the RNA binding activity of the Lsm1-7–Pat1 complex', *RNA*, 20(9), pp. 1465–1475. Available at: https://doi.org/10.1261/rna.045252.114.

Chowdhury, A., Mukhopadhyay, J. and Tharun, S. (2007) 'The decapping activator Lsm1p-7p–Pat1p complex has the intrinsic ability to distinguish between oligoadenylated and polyadenylated RNAs', *RNA*, 13(7), pp. 998–1016. Available at: https://doi.org/10.1261/rna.502507.

Cooper, M., Johnston, L.H. and Beggs, J.D. (1995) 'Identification and characterization of Uss1p (Sdb23p): a novel U6 snRNA-associated protein with significant similarity to core proteins of small nuclear ribonucleoproteins.', *The EMBO Journal*, 14(9), pp. 2066–2075.

Costanzo, M. *et al.* (2010) 'The genetic landscape of a cell', *Science (New York, N.Y.)*, 327(5964), pp. 425–431. Available at: https://doi.org/10.1126/science.1180823.

Decker, C.J., Teixeira, D. and Parker, R. (2007) 'Edc3p and a glutamine/asparagine-rich domain of Lsm4p function in processing body assembly in Saccharomyces cerevisiae', *The Journal of Cell Biology*, 179(3), pp. 437–449. Available at: https://doi.org/10.1083/jcb.200704147.

Delorme-Axford, E. and Klionsky, D.J. (2019) 'On the edge of degradation: Autophagy regulation by RNA decay', *Wiley interdisciplinary reviews. RNA*, 10(3), p. e1522. Available at: https://doi.org/10.1002/wrna.1522.

DiCarlo, J.E. *et al.* (2013) 'Genome engineering in Saccharomyces cerevisiae using CRISPR-Cas systems', *Nucleic Acids Research*, 41(7), pp. 4336–4343. Available at: https://doi.org/10.1093/nar/gkt135.

Eisenberg, T. *et al.* (2009) 'Induction of autophagy by spermidine promotes longevity', *Nature Cell Biology*, 11(11), pp. 1305–1314. Available at: https://doi.org/10.1038/ncb1975.

Fabrizio, P. and Longo, V.D. (2003) 'The chronological life span of Saccharomyces cerevisiae', *Aging Cell*, 2(2), pp. 73–81. Available at: https://doi.org/10.1046/j.1474-9728.2003.00033.x.

Fontana, L., Partridge, L. and Longo, V.D. (2010) 'Extending Healthy Life Span—From Yeast to Humans', *Science*, 328(5976), pp. 321–326. Available at: https://doi.org/10.1126/science.1172539.

Gatica, D. *et al.* (2019) 'The Pat1-Lsm complex prevents 3′ to 5′ degradation of a specific subset of ATG mRNAs during nitrogen starvation-induced autophagy', *Autophagy*, 15(4), pp. 750–751. Available at: https://doi.org/10.1080/15548627.2019.1587262.

Geng, J. *et al.* (2008) 'Quantitative analysis of autophagy-related protein stoichiometry by fluorescence microscopy', *The Journal of Cell Biology*, 182(1), pp. 129–140. Available at: https://doi.org/10.1083/jcb.200711112.

Geng, J. and Klionsky, D.J. (2008) 'The Atg8 and Atg12 ubiquitin-like conjugation systems in macroautophagy. 'Protein Modifications: Beyond the Usual Suspects' Review Series', *EMBO Reports*, 9(9), pp. 859–864. Available at: https://doi.org/10.1038/embor.2008.163.

Gibson, R.K. and Peberdy, J.F. (1972) 'Fine structure of protoplasts of Aspergillus nidulans', *Journal of General Microbiology*, 72(3), pp. 529–538. Available at: https://doi.org/10.1099/00221287-72-3-529.

Gietz, R.D. and Woods, R.A. (2006) 'Yeast Transformation by the LiAc/SS Carrier DNA/PEG Method', in W. Xiao (ed.) *Yeast Protocol*. Totowa, NJ: Humana Press (Methods in Molecular Biology), pp. 107–120. Available at: https://doi.org/10.1385/1-59259-958-3:107.

Goldberg, A.A. *et al.* (2009) 'Effect of calorie restriction on the metabolic history of chronologically aging yeast', *Experimental Gerontology*, 44(9), pp. 555–571. Available at: https://doi.org/10.1016/j.exger.2009.06.001.

Guarente, L. (1999) 'Diverse and dynamic functions of the Sir silencing complex', *Nature Genetics*, 23(3), pp. 281–285. Available at: https://doi.org/10.1038/15458.

Guhaniyogi, J. and Brewer, G. (2001) 'Regulation of mRNA stability in mammalian cells', *Gene*, 265(1–2), pp. 11–23. Available at: https://doi.org/10.1016/s0378-1119(01)00350-x.

Gwinn, D.M. *et al.* (2008) 'AMPK phosphorylation of raptor mediates a metabolic checkpoint', *Molecular cell*, 30(2), pp. 214–226. Available at: https://doi.org/10.1016/j.molcel.2008.03.003.

He, W. and Parker, R. (2000) 'Functions of Lsm proteins in mRNA degradation and splicing', *Current Opinion in Cell Biology*, 12(3), pp. 346–350. Available at: https://doi.org/10.1016/s0955-0674(00)00098-3.

He, W. and Parker, R. (2001) 'The yeast cytoplasmic LsmI/Pat1p complex protects mRNA 3' termini from partial degradation', *Genetics*, 158(4), pp. 1445–1455. Available at: https://doi.org/10.1093/genetics/158.4.1445.

Hernández-Elvira, M. and Sunnerhagen, P. (2022) 'Post-transcriptional regulation during stress', *FEMS Yeast Research*, 22(1), p. foac025. Available at: https://doi.org/10.1093/femsyr/foac025.

Hu, G. *et al.* (2015) 'A conserved mechanism of TOR-dependent RCK-mediated mRNA degradation regulates autophagy', *Nature Cell Biology*, 17(7), pp. 930–942. Available at: https://doi.org/10.1038/ncb3189.

Inoki, K., Zhu, T. and Guan, K.-L. (2003) 'TSC2 mediates cellular energy response to control cell growth and survival', *Cell*, 115(5), pp. 577–590. Available at: https://doi.org/10.1016/s0092-8674(03)00929-2.

Iwama, R. and Ohsumi, Y. (2019) 'Analysis of autophagy activated during changes in carbon source availability in yeast cells', *The Journal of Biological Chemistry*, 294(14), pp. 5590–5603. Available at: https://doi.org/10.1074/jbc.RA118.005698.

Kabani, M. and Melki, R. (2016) 'More than just trash bins? Potential roles for extracellular vesicles in the vertical and horizontal transmission of yeast prions', *Current Genetics*, 62(2), pp. 265–270. Available at: https://doi.org/10.1007/s00294-015-0534-6.

Kaeberlein, M., McVey, M. and Guarente, L. (1999) 'The SIR2/3/4 complex and SIR2 alone promote longevity in Saccharomyces cerevisiae by two different mechanisms', *Genes & Development*, 13(19), pp. 2570–2580.

Kato, M. *et al.* (2012) 'Cell-free formation of RNA granules: low complexity sequence domains form dynamic fibers within hydrogels', *Cell*, 149(4), pp. 753–767. Available at: https://doi.org/10.1016/j.cell.2012.04.017.

Kirisako, T. *et al.* (1999) 'Formation Process of Autophagosome Is Traced with Apg8/Aut7p in Yeast', *The Journal of Cell Biology*, 147(2), pp. 435–446.

Klionsky, Daniel J *et al.* (2021) 'Autophagy in major human diseases', *The EMBO Journal*, 40(19), p. e108863. Available at: https://doi.org/10.15252/embj.2021108863.

Klionsky, Daniel J. *et al.* (2021) 'Guidelines for the use and interpretation of assays for monitoring autophagy (4th edition)1', *Autophagy*, 17(1), pp. 1–382. Available at: https://doi.org/10.1080/15548627.2020.1797280.

Klionsky, D.J. and Emr, S.D. (2000) 'Autophagy as a Regulated Pathway of Cellular Degradation', *Science (New York, N.Y.)*, 290(5497), pp. 1717–1721.

Kumar, P. *et al.* (2019) 'Inhibition of TOR signalling in lea1 mutant induces apoptosis in Saccharomyces cerevisiae', *Annals of Microbiology*, 69(4), pp. 341–352. Available at: https://doi.org/10.1007/s13213-018-1422-3.

Landry, J. *et al.* (2000) 'The silencing protein SIR2 and its homologs are NAD-dependent protein deacetylases', *Proceedings of the National Academy of Sciences of the United States of America*, 97(11), pp. 5807–5811.

Lei, Y. *et al.* (2022) 'How Cells Deal with the Fluctuating Environment: Autophagy Regulation under Stress in Yeast and Mammalian Systems', *Antioxidants*, 11(2), p. 304. Available at: https://doi.org/10.3390/antiox11020304.

Liu, X. *et al.* (2019) 'Bidirectional roles of Dhh1 in regulating autophagy', *Autophagy*, 15(10), pp. 1838–1839. Available at: https://doi.org/10.1080/15548627.2019.1621632.

Madeo, F., Fröhlich, E. and Fröhlich, K.-U. (1997) 'A Yeast Mutant Showing Diagnostic Markers of Early and Late Apoptosis', *The Journal of Cell Biology*, 139(3), pp. 729–734.

Mayes, A.E. *et al.* (1999) 'Characterization of Sm-like proteins in yeast and their association with U6 snRNA', *The EMBO Journal*, 18(15), pp. 4321–4331. Available at: https://doi.org/10.1093/emboj/18.15.4321.

Mazzoni, C., Mancini, P., Madeo, F., *et al.* (2003) 'A Kluyveromyces lactis mutant in the essential gene KlLSM4 shows phenotypic markers of apoptosis', *FEMS yeast research*, 4(1), pp. 29–35. Available at: https://doi.org/10.1016/S1567-1356(03)00151-X.

Mazzoni, C., Mancini, P., Verdone, L., *et al.* (2003) 'A Truncated Form of KlLsm4p and the Absence of Factors Involved in mRNA Decapping Trigger Apoptosis in Yeast', *Molecular Biology of the Cell*. Edited by M.P. Wickens, 14(2), pp. 721–729. Available at: https://doi.org/10.1091/mbc.e02-05-0258.

Mazzoni, C. *et al.* (2005) 'Yeast caspase 1 links messenger RNA stability to apoptosis in yeast', *EMBO reports*, 6(11), pp. 1076–1081. Available at: https://doi.org/10.1038/sj.embor.7400514.

Mazzoni, C., D'Addario, I. and Falcone, C. (2007) 'The C-terminus of the yeast Lsm4p is required for the association to P-bodies', *FEBS Letters*, 581(25), pp. 4836–4840. Available at: https://doi.org/10.1016/j.febslet.2007.09.009.

Mazzoni, C. and Falcone, C. (2011) 'mRNA stability and control of cell proliferation', *Biochemical Society Transactions*, 39(5), pp. 1461–1465. Available at: https://doi.org/10.1042/BST0391461.

Medvedik, O. *et al.* (2007) 'MSN2 and MSN4 Link Calorie Restriction and TOR to Sirtuin-Mediated Lifespan Extension in Saccharomyces cerevisiae', *PLOS Biology*, 5(10), p. e261. Available at: https://doi.org/10.1371/journal.pbio.0050261.

Mitchell, S.F. *et al.* (2013) 'Global analysis of yeast mRNPs', *Nature Structural & Molecular Biology*, 20(1), pp. 127–133. Available at: https://doi.org/10.1038/nsmb.2468.

Morselli, E. *et al.* (2010) 'Caloric restriction and resveratrol promote longevity through the Sirtuin-1-dependent induction of autophagy', *Cell Death & Disease*, 1(1), p. e10. Available at: https://doi.org/10.1038/cddis.2009.8.

Nakatogawa, H. (2015) 'Regulated degradation: controlling the stability of autophagy gene transcripts', *Developmental Cell*, 34(2), pp. 132–134. Available at: https://doi.org/10.1016/j.devcel.2015.07.002.

Noda, T. and Ohsumi, Y. (1998) 'Tor, a phosphatidylinositol kinase homologue, controls autophagy in yeast', *The Journal of Biological Chemistry*, 273(7), pp. 3963–3966. Available at: https://doi.org/10.1074/jbc.273.7.3963.

Obara, K. *et al.* (2008) 'The Atg18-Atg2 Complex Is Recruited to Autophagic Membranes via Phosphatidylinositol 3-Phosphate and Exerts an Essential Function', *The Journal of Biological Chemistry*, 283(35), pp. 23972–23980. Available at: https://doi.org/10.1074/jbc.M803180200.

O'Grady, T. *et al.* (2022) 'Sorting and packaging of RNA into extracellular vesicles shape intracellular transcript levels', *BMC Biology*, 20(1), p. 72. Available at: https://doi.org/10.1186/s12915-022-01277-4.

Okamoto, K., Kondo-Okamoto, N. and Ohsumi, Y. (2009) 'Mitochondria-anchored receptor Atg32 mediates degradation of mitochondria via selective autophagy', *Developmental Cell*, 17(1), pp. 87–97. Available at: https://doi.org/10.1016/j.devcel.2009.06.013.

Onodera, J. and Ohsumi, Y. (2005) 'Autophagy is required for maintenance of amino acid levels and protein synthesis under nitrogen starvation', *The Journal of Biological Chemistry*, 280(36), pp. 31582–31586. Available at: https://doi.org/10.1074/jbc.M506736200.

Palermo, V. *et al.* (2015) 'NEM1 acts as a suppressor of apoptotic phenotypes in LSM4 yeast mutants', *FEMS Yeast Research*, 15(fov074). Available at: https://doi.org/10.1093/femsyr/fov074.

Palermo, V., Falcone, C. and Mazzoni, C. (2007) 'Apoptosis and aging in mitochondrial morphology mutants of S. cerevisiae', *Folia Microbiologica*, 52(5), pp. 479–483. Available at: https://doi.org/10.1007/BF02932107.

Peres da Silva, R. *et al.* (2015) 'Extracellular vesicle-mediated export of fungal RNA', *Scientific Reports*, 5(1), p. 7763. Available at: https://doi.org/10.1038/srep07763.

Pérez-Pérez, M.E. *et al.* (2014) 'The yeast autophagy protease Atg4 is regulated by thioredoxin', *Autophagy*, 10(11), pp. 1953–1964. Available at: https://doi.org/10.4161/auto.34396.

Poljak, A. *et al.* (2003) 'Oxidative damage to proteins in yeast cells exposed to adaptive levels of H(2)O(2)', *Redox Report: Communications in Free Radical Research*, 8(6), pp. 371–377. Available at: https://doi.org/10.1179/135100003225003401.

Rahman, M.A., Mostofa, M.G. and Ushimaru, T. (2018) 'The Nem1/Spo7-Pah1/lipin axis is required for autophagy induction after TORC1 inactivation', *The FEBS journal*, 285(10), pp. 1840–1860. Available at: https://doi.org/10.1111/febs.14448.

Rajendran, L. *et al.* (2014) 'Emerging Roles of Extracellular Vesicles in the Nervous System', *The Journal of Neuroscience*, 34(46), pp. 15482–15489. Available at: https://doi.org/10.1523/JNEUROSCI.3258-14.2014.

Ramya, V. and Rajasekharan, R. (2016) 'ATG15 encodes a phospholipase and is transcriptionally regulated by YAP1 in Saccharomyces cerevisiae', *FEBS Letters*, 590(18), pp. 3155–3167. Available at: https://doi.org/10.1002/1873-3468.12369.

Reijns, M.A.M. *et al.* (2008) 'A role for Q/N-rich aggregation-prone regions in P-body localization', *Journal of Cell Science*, 121(Pt 15), pp. 2463–2472. Available at: https://doi.org/10.1242/jcs.024976.

Reis, F.C.G. *et al.* (2019) 'A Novel Protocol for the Isolation of Fungal Extracellular Vesicles Reveals the Participation of a Putative Scramblase in Polysaccharide Export and Capsule Construction in Cryptococcus gattii', *mSphere*, 4(2), pp. e00080-19. Available at: https://doi.org/10.1128/mSphere.00080-19.

Rodrigues, M.L. *et al.* (2011) 'Vesicular transport systems in fungi', *Future microbiology*, 6(11), pp. 1371–1381. Available at: https://doi.org/10.2217/fmb.11.112.

Ryter, S.W., Cloonan, S.M. and Choi, A.M.K. (2013) 'Autophagy: A Critical Regulator of Cellular Metabolism and Homeostasis', *Molecules and Cells*, 36(1), pp. 7–16. Available at: https://doi.org/10.1007/s10059-013-0140-8.

Sampaio-Marques, B. *et al.* (2012) 'SNCA (α-synuclein)-induced toxicity in yeast cells is dependent on sirtuin 2 (Sir2)-mediated mitophagy', *Autophagy*, 8(10), pp. 1494–1509. Available at: https://doi.org/10.4161/auto.21275.

Schneider, C.A., Rasband, W.S. and Eliceiri, K.W. (2012) 'NIH Image to ImageJ: 25 years of image analysis', *Nature Methods*, 9(7), pp. 671–675. Available at: https://doi.org/10.1038/nmeth.2089.

Singh, A.K. *et al.* (2019) 'Rapamycin Confers Neuroprotection Against Aging-Induced Oxidative Stress, Mitochondrial Dysfunction, and Neurodegeneration in Old Rats Through Activation of Autophagy', *Rejuvenation Research*, 22(1), pp. 60–70. Available at: https://doi.org/10.1089/rej.2018.2070.

Stovicek, V., Borodina, I. and Forster, J. (2015) 'CRISPR–Cas system enables fast and simple genome editing of industrial Saccharomyces cerevisiae strains', *Metabolic Engineering Communications*, 2, pp. 13–22. Available at: https://doi.org/10.1016/j.meteno.2015.03.001.

Suchorska, W. and Lach, M. (2015) 'The role of exosomes in tumor progression and metastasis (Review)', *Oncology Reports*, 35, pp. 1237–1244. Available at: https://doi.org/10.3892/or.2015.4507.

Sun, Z.-P., Tan, Z.-G. and Peng, C. (2022) 'Long noncoding RNA LINC01419 promotes hepatocellular carcinoma malignancy by mediating miR-485-5p/LSM4 axis', *The Kaohsiung Journal of Medical Sciences*, 38(9), pp. 826–838. Available at: https://doi.org/10.1002/kjm2.12566.

Suzuki, S.W., Onodera, J. and Ohsumi, Y. (2011) 'Starvation induced cell death in autophagy-defective yeast mutants is caused by mitochondria dysfunction', *PloS One*, 6(2), p. e17412. Available at: https://doi.org/10.1371/journal.pone.0017412.

Ta, H.D.K. *et al.* (2021) 'Potential Therapeutic and Prognostic Values of LSM Family Genes in Breast Cancer', *Cancers*, 13(19), p. 4902. Available at: https://doi.org/10.3390/cancers13194902.

Takeshige, K. *et al.* (1992) 'Autophagy in yeast demonstrated with proteinase-deficient mutants and conditions for its induction.', *Journal of Cell Biology*, 119(2), pp. 301–311. Available at: https://doi.org/10.1083/jcb.119.2.301.

Taylor, R.G., Walker, D.C. and McInnes, R.R. (1993) 'E. coli host strains significantly affect the quality of small scale plasmid DNA preparations used for sequencing.', *Nucleic Acids Research*, 21(7), pp. 1677–1678.

Tharun, S. *et al.* (2000) 'Yeast Sm-like proteins function in mRNA decapping and decay', *Nature*, 404(6777), pp. 515–518. Available at: https://doi.org/10.1038/35006676.

Tharun, S. *et al.* (2005) 'Mutations in the Saccharomyces cerevisiae LSM1 gene that affect mRNA decapping and 3' end protection', *Genetics*, 170(1), pp. 33–46. Available at: https://doi.org/10.1534/genetics.104.034322.

Tsukada, M. and Ohsumi, Y. (1993) 'Isolation and characterization of autophagy-defective mutants of Saccharomyces cerevisiae', *FEBS letters*, 333(1–2), pp. 169–174. Available at: https://doi.org/10.1016/0014-5793(93)80398-e.

Wilusz, C.J. and Wilusz, J. (2013) 'Lsm proteins and Hfq: Life at the 3' end', *RNA biology*, 10(4), pp. 592–601. Available at: https://doi.org/10.4161/rna.23695.

Yin, Z. *et al.* (2023) 'Bidirectional roles of the Ccr4-Not complex in regulating autophagy before and after nitrogen starvation', *Autophagy*, 19(2), pp. 415–425. Available at: https://doi.org/10.1080/15548627.2022.2036476.

Zhao, K. *et al.* (2019) 'Extracellular vesicles secreted by Saccharomyces cerevisiae are involved in cell wall remodelling', *Communications Biology*, 2(1), pp. 1–13. Available at: https://doi.org/10.1038/s42003-019-0538-8.

9. Supplemental Figures

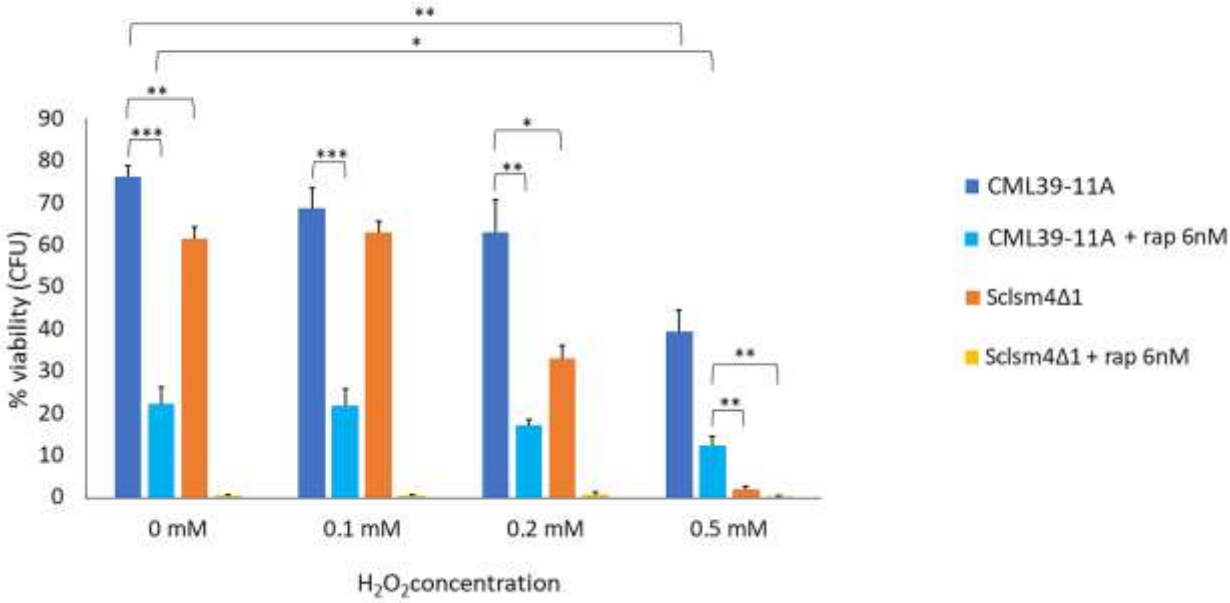

Supplemental Figure 1. Cell viability was calculated as the percentage of microcolony forming cells. Data are represented as the mean of three independent experiments ± standard deviation. *p-value <0.05, **p-value <0.01***p-value<0.001.

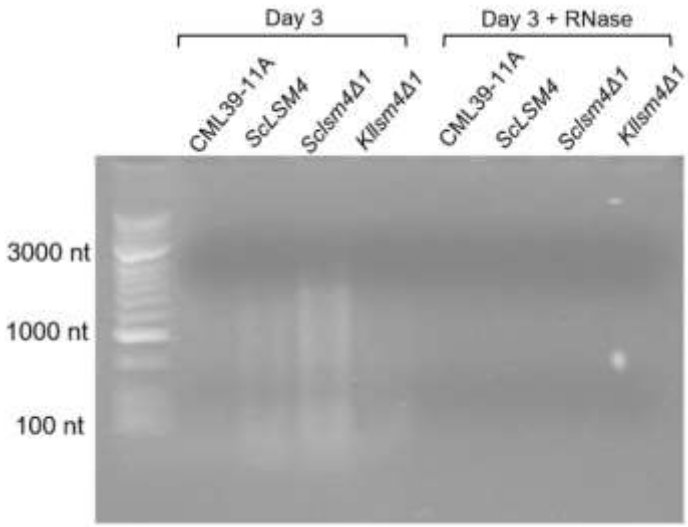

Supplemental Figure 2. Electrophoresis analysis on agarose gel of supernatant RNAs after 3 days of culture in water of the strains of interest. Treatment with RNase was used to verify the nature of the nucleic acid.

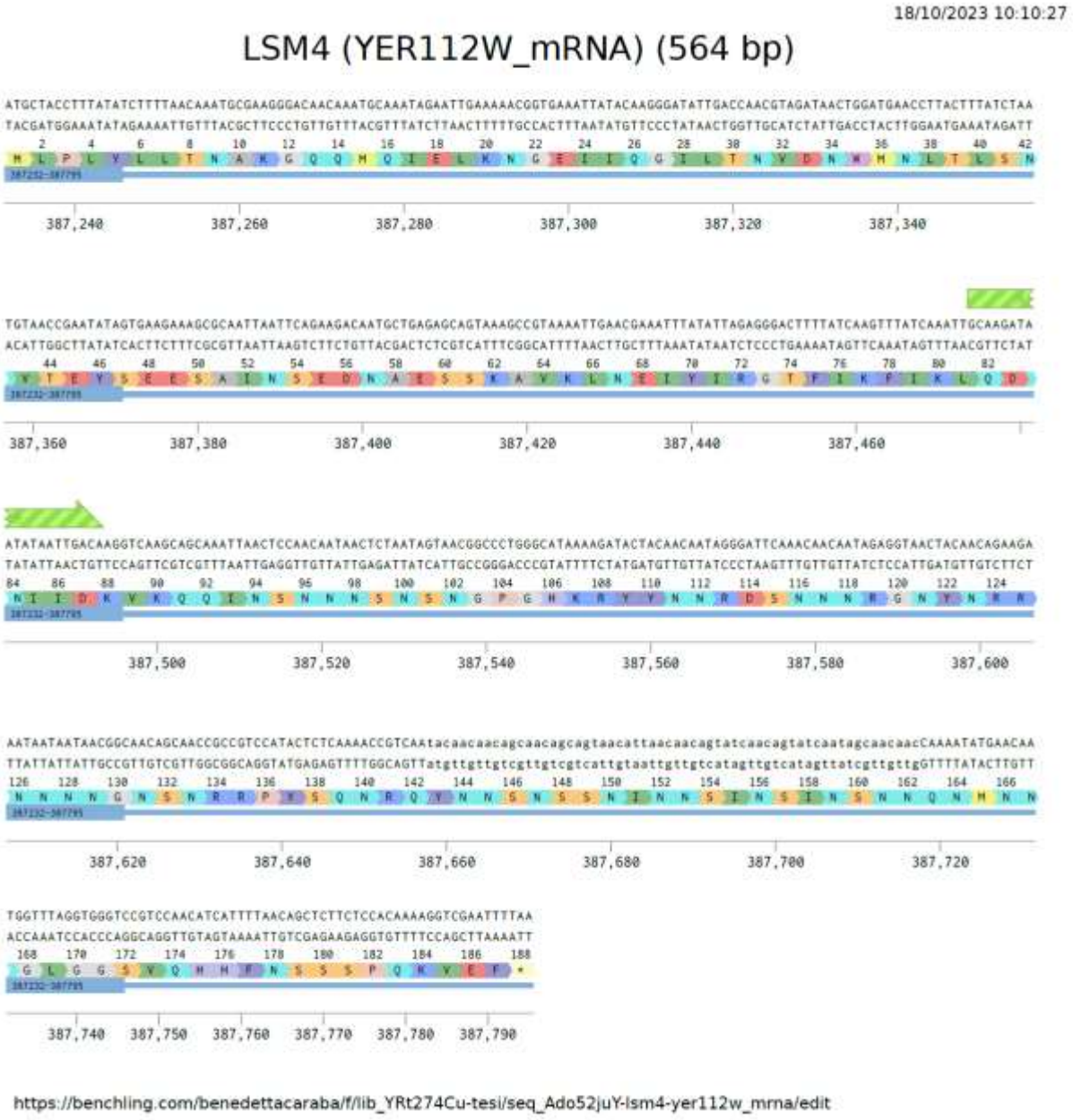

Supplemental Figure 3. The gRNA of interest was found using the bioinformatic tool Benchling © and it is represented with the green arrow. The PAM sequence (AGG) is right after the 87th aminoacid, allowing us to design the donor DNA of interest to recreate the truncated form of Lsm4 fused to the reporter protein GFP. The values of the on-target score is 67.00 and the off-target score is 98.00.

Supplemental Figure 4. Sequencing results of the cloned pCfB2311-Lsm4Δ1-GFP plasmid show the correct substitution of the gRNA.

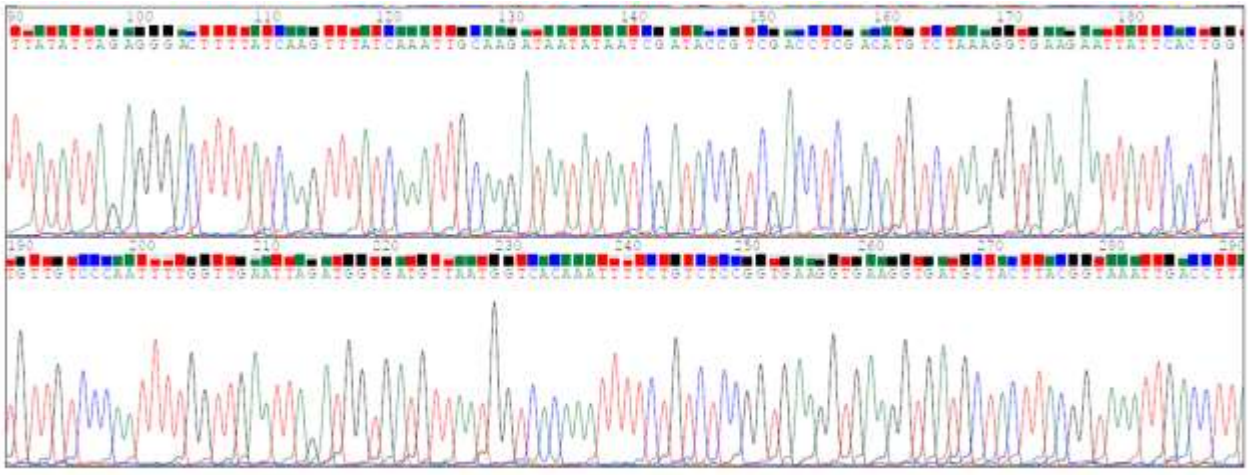

Supplemental Figure 5. Sequencing of the control PCR fragments shows the correct integration of the Lsm4Δ1-GFP cassette in the desired site.

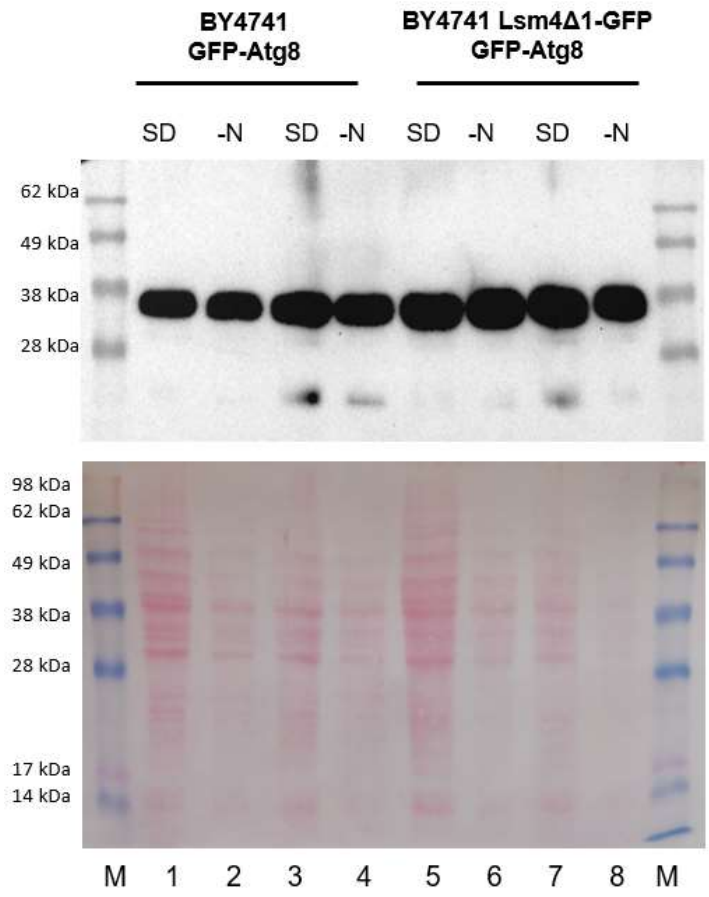

Supplemental Figure 6. Western Blot analysis on BY4741/pUG36-*ATG8* and BY4741 *lsm4Δ1*-GFP/pUG36-*ATG8* strains after 4 hours (lanes 1, 2, 5 and 6) and 20 hours (3, 4, 7 and 8) in nutrient rich (SD) and under nitrogen starvation (SD-N). The GFP-Atg8 protein signal (41 kDa) is too intense to distinguish the *lsm4Δ1*-GFP band (36.44 kDa). One of three different experiments is shown.

10. List of publications

- Caraba B, Stirpe M, Palermo V, Vaccher U, Bianchi MM, Falcone C, Mazzoni C. **Yeast Lsm Pro-Apoptotic Mutants Show Defects in Autophagy**. Int J Mol Sci. 2023 Sep 5;24(18):13708. doi: 10.3390/ijms241813708. PMID: 37762007; PMCID: PMC10530990.

- Caraba B, Stirpe M, Palermo V, Vaccher U, Bianchi MM, Falcone C, Mazzoni C. **Calorie restriction suppresses premature aging in pro-apoptotic yeast mutants** (in preparation)

- Palermo V, Caraba B, Martins Fraguas R, Materazzi S, Risoluti R, Mazzoni C. **The powerful effect of two tropical fruits from brazilian savannah on yeast aging as a longlife elixir** (in preparation)